

# BRIDGING THEORY AND PRACTICE: STATISTICAL INFERENCE FOR LATENT SPACE MODELS OF NETWORKS

BY YUANG TIAN<sup>1,a</sup>, JIAJIN SUN<sup>2,b</sup> AND YINQIU HE<sup>3,c</sup>

<sup>1</sup>*Department of Mathematics, Hong Kong University of Science and Technology, [yatian@ust.hk](mailto:yatian@ust.hk)*

<sup>2</sup>*Department of Statistics, Florida State University, [jsum5@fsu.edu](mailto:jsum5@fsu.edu)*

<sup>3</sup>*Department of Statistics, University of Wisconsin-Madison, [yinqiu.he@wisc.edu](mailto:yinqiu.he@wisc.edu)*

Latent space models have been widely adopted in modeling network data. Developing statistical inference for estimated model parameters enables quantifying associated uncertainty and is pivotal for downstream tasks. Despite recent progress on statistical inference of maximum likelihood estimation, crucial gaps remain between asymptotic theoretical guarantees and practical use. Specifically, how are the oracle maximum likelihood estimators related to the solutions produced by algorithms in practice? Can rigorous guarantees be established for existing algorithms without unnecessary restrictions? To address these fundamental questions, we develop a unified analytical framework that bridges theory and practice of statistical inference for latent space models. First, for the maximum likelihood estimation, we relax the spectral-multiplicity constraint in the existing asymptotic theory to broaden the applicability. Second, we overcome the dependence on unknown true parameters in prior algorithmic analyses by developing novel adaptive criteria and theoretical tools. For the widely used algorithm based on the projected gradient descent and the singular value thresholding, we explicitly connect their outputs to the maximum likelihood estimator without relying on unknown information. Our results provide a solid foundation for practically useful and statistically principled statistical inference in network analysis.

**1. Introduction.** Networks encode relational information between entities in complex systems and have become ubiquitous across various scientific domains [33], including social science [20, 30], economics [6], neuroscience [45, 46], and biomedical studies [26]. In most settings, a network can be represented as a graph consisting of a set of nodes and a set of edges, which encode the entities in the system and the interactions between them, respectively.

To capture complex edge dependence and other structural characteristics in networks, latent space modeling is one of the widely used approaches [3, 15, 25, 34]. The central idea is to associate each node with a low-dimensional vector in the latent space. The relational structure between two nodes, such as their connecting probability or weighted edge value, can then be characterized by a kernel function of latent vectors. One common choice of the kernel function is the inner product between latent vectors, which can capture important network features, such as transitivity, reciprocity, and community structures [3, 4, 11, 18, 19, 22, 24, 35, 50].

In this work, we study statistical inference of the latent vectors. Estimated latent vectors are often used for interpretation and visualization to investigate fundamental structures underlying networks. Quantifying their uncertainty is therefore essential for drawing uncertainty-aware conclusions in downstream tasks that rely on these estimates, including vertex clustering [31], network-based regression [13, 27], testing for networks [37], and link prediction

---

*MSC2020 subject classifications.* Primary 62H12, 05C50; secondary 91D30, 62F12, 62F30.

*Keywords and phrases.* Network analysis, Latent space models, Maximum likelihood estimation, Non-convex optimization.

[29]. Nevertheless, inference for latent vectors poses unique challenges that the number of unknown vectors grows with respect to the network size, and these vectors themselves are inherently unidentifiable.

In the existing literature, one research line focuses on the random dot product graphs (RDPG) [48] and studies the asymptotic distributions of spectral estimators [2, 36, 38]. Meanwhile, [47] show that spectral embeddings do not fully exploit the Bernoulli sampling likelihood information and could therefore be suboptimal in terms of asymptotic covariance matrices. To address this, [47] propose an efficient one-step update based on solving likelihood-based estimating equations and demonstrate improved efficiency under the RDPG model.

Another line of research considers a broad class of latent space models with general link functions. In this setting, [19] establish uniform consistency and asymptotic distributions for the maximum likelihood estimators of the latent vectors. Technically, to handle the non-identifiability of latent vectors, they introduce a Lagrange-type penalty function. Computationally, [19] solve the maximum likelihood estimators by the two-stage approach proposed in [22], which utilizes universal singular value thresholding [8] for initialization, followed by the projected gradient descent for optimization. Despite these advances, an important gap remains between the available inferential theory and the algorithms used in practice. In particular, it is unclear whether the estimator produced by the algorithm in [22] coincides with the constrained maximum likelihood estimator defined in [19], putting a question on applying the inferential results in practice.

This gap cannot be directly addressed by existing developments and poses unique challenges. First, the analysis in [19] assumes that the matrix of latent vectors has non-vanishing eigengaps among all non-zero eigenvalues, and that the likelihood is maximized within a bounded region containing the true parameters. However, these assumptions can be difficult to verify or implement because the ground truth is unknown in practice. Second, [19] examine a Lagrange-type penalized log-likelihood function, whereas the gradient descent algorithm in [22] directly operates on the unpenalized log-likelihood. This mismatch is especially important because the original likelihood for latent vectors is nonconvex. Consequently, unlike in convex problems, there is no default link between the ideal maximum likelihood estimator and the output of the optimization algorithm. Third, the original algorithmic formulation in [22] includes impractical or seemingly unnecessary steps to reach theoretical guarantee of convergence. For example, [22] point out that the step of projecting parameters onto unknown bounded sets is unnecessary in practice, even though it is required in its theoretical analysis. In addition, convergence guarantees require tuning parameters, such as the projection set used in singular value thresholding and the step size in gradient descent, to be chosen appropriately. In general, however, suitable choices of these quantities depend on unknown model parameters and are therefore infeasible in practice.

In this work, we examine the maximum likelihood estimation of latent vectors under the class of latent space models considered in [22] and [19]. Our goal is to build a rigorous bridge between the practical computation of the constrained maximum likelihood estimator (MLE) and the inferential theory developed for its idealized formulation. Specifically, our main contributions are summarized as follows.

1. *MLE inferential theory.* We develop a unified inferential framework for the constrained MLE of latent vectors. A key feature of our theory is that it surpasses the spectral restrictions commonly imposed in the existing literature.
2. *Data-adaptive algorithms.* For the widely-used two-stage algorithm, we develop novel adaptive adjustments that eliminate their dependence on unknown true model parameters. In particular, we develop new adaptive line search conditions for selecting appropriate step sizes and rigorously justify skipping the projection onto unknown constraint sets in the gradient descent algorithm. Moreover, we develop a range-adaptive singular value thresholding for the initialization that can be applied to both bounded and unbounded settings.

3. *Bridging MLE and algorithms.* We build explicit connections between the constrained MLE and the outputs of practical algorithms. Notably, we show that although the definition of the constrained MLE relies on the true parameters, the practical algorithm can approximate this estimator under suitable conditions without access to those true parameters. Our analysis directly examines solutions of the non-penalized likelihood maximization and does not rely on additional transformations.

The rest of this paper is organized as follows. Section 2 introduces the class of latent space models under consideration and the problem setup. Section 3 explains the gaps between existing theoretical and algorithmic frameworks in detail. Section 4 presents our new asymptotic theory for the maximum likelihood estimators, while guarantees on practical algorithms are given in Section 5. Sections 6 and 7 present simulation studies and a data analysis, respectively. Additional numerical results and all proofs are deferred to the Supplementary Material.

*Notation.* Let  $\mathbb{R}$  and  $\mathbb{N}$  denote the sets of the real numbers and the natural numbers, respectively. Given two sequences of real numbers  $\{g_n\}$  and  $\{h_n\}$ , the notation  $g_n \lesssim h_n$  means that there exists a constant  $c > 0$  such that  $g_n \leq ch_n$ ;  $g_n \asymp h_n$  means  $h_n \lesssim g_n$  and  $g_n \lesssim h_n$  simultaneously;  $g_n \ll h_n$  indicates that  $\lim_{n \rightarrow \infty} g_n/h_n = 0$ . For vectors  $x = (x_i)_{i=1}^n$  and  $y = (y_i)_{i=1}^n \in \mathbb{R}^n$ , define their inner product as  $\langle x, y \rangle = \sum_{i=1}^n x_i y_i$ , the two norm as  $\|x\|_2 = \sqrt{\langle x, x \rangle}$ , and the infinity norm as  $\|x\|_\infty = \max_{1 \leq i \leq n} |x_i|$ . For matrices  $X = (x_{ij})_{1 \leq i \leq n, 1 \leq j \leq m}$  and  $Y = (y_{ij})_{1 \leq i \leq n, 1 \leq j \leq m} \in \mathbb{R}^{n \times m}$ , define their inner product as  $\langle X, Y \rangle = \sum_{i=1}^n \sum_{j=1}^m x_{ij} y_{ij}$ , the Frobenius norm as  $\|X\|_F = \sqrt{\langle X, X \rangle}$ , the operator norm as  $\|X\|_{\text{op}} = \sup_{\|v\|_2=1} \|Xv\|_2$ , and the two-to-infinity norm as  $\|X\|_{2 \rightarrow \infty} = \sup_{\|v\|_2=1} \|Xv\|_\infty$ . For matrices  $X_1, \dots, X_p$ , let  $\text{blkdiag}(X_1, \dots, X_p)$  be the block-diagonal matrix with  $X_1, \dots, X_p$  on its diagonal. Let  $I_k$  denote  $k \times k$  identity matrix, and  $\mathcal{O}(k) = \{Q \in \mathbb{R}^{k \times k} : QQ^\top = I_k\}$  represent the set of  $k \times k$  orthogonal transformation matrices. For a square matrix  $X \in \mathbb{R}^{n \times n}$ , let  $\text{vech}(X) = (X_{12}, X_{13}, \dots, X_{n-1,n})^\top \in \mathbb{R}^{n(n-1)/2}$  be the vectorization of its strictly upper-triangular entries.

**2. Latent Space Model.** Consider an undirected network of  $n$  nodes, encoded by a symmetric adjacency matrix  $A = (A_{ij})_{1 \leq i, j \leq n}$  where each  $A_{ij}$  represents the connection between two nodes  $i$  and  $j \in \{1, \dots, n\}$  and  $A_{ii} = 0$  indicating no self loops. For binary networks,  $A_{ij} = 1$  means that two nodes  $i$  and  $j$  are connected, and zero otherwise [22]. For weighted networks,  $A_{ij}$  represents the weight of the edge connecting two nodes  $i$  and  $j$  [14, 40]. In applications, networks may contain binary, continuous, or count-valued edge weights. Latent space modeling assumes that each node  $i$  is associated with a latent vector  $z_i \in \mathbb{R}^k$  and a degree heterogeneity parameter  $\alpha_i \in \mathbb{R}$ . Then for any  $1 \leq i < j \leq n$ ,

$$(1) \quad A_{ij} = A_{ji} \sim p(\cdot \mid \Theta_{ij}) \quad \text{independently with} \quad \Theta_{ij} = \alpha_i + \alpha_j + \langle z_i, z_j \rangle,$$

where  $p(\cdot \mid \theta)$  denotes the probability density/mass function with a one-dimensional parameter  $\theta$ . Let  $Z = [z_1, \dots, z_n]^\top \in \mathbb{R}^{n \times k}$  and  $\alpha = [\alpha_1, \dots, \alpha_n]^\top \in \mathbb{R}^n$  represent the parameters in matrix form. We can also write a matrix form  $\Theta := (\Theta_{ij})_{1 \leq i, j \leq n} = ZZ^\top + \alpha 1_n^\top + 1_n \alpha^\top$  if we extend the definition of  $\Theta_{ij}$  to the case  $i \geq j$  in the same way as in (1), where  $1_n$  is the all-ones vector in  $\mathbb{R}^n$ . Such a matrix form has also been discussed in [22].

In this work, we assume that the observed data are generated by fixed true parameters  $Z^* = [z_1^*, \dots, z_n^*]^\top \in \mathbb{R}^{n \times k}$  and  $\alpha^* = [\alpha_1^*, \dots, \alpha_n^*]^\top \in \mathbb{R}^n$ . Our goal is to estimate these true parameters and quantify the associated uncertainty. However,  $(Z^*, \alpha^*)$  is not uniquely identifiable under the model (1). Given  $(Z^*, \alpha^*)$ , we can choose any  $Q \in \mathcal{O}(k)$  and  $c \in \mathbb{R}^k$  to construct transformed parameters

$$(2) \quad \tilde{z}_i = Q(z_i^* - c) \quad \text{and} \quad \tilde{\alpha}_i = \alpha_i^* + (c^\top z_i^* - \|c\|_2^2/2) \quad \text{for all } 1 \leq i \leq n,$$

satisfying  $\text{vech}(\Theta^*) = \text{vech}(\tilde{\Theta})$ , i.e.,  $\alpha_i^* + \alpha_j^* + \langle z_i^*, z_j^* \rangle = \tilde{\alpha}_i + \tilde{\alpha}_j + \langle \tilde{z}_i, \tilde{z}_j \rangle$  for all  $1 \leq i < j \leq n$ . By the model formulation in (1), we know  $(Z^*, \alpha^*)$  and  $(\tilde{Z}, \tilde{\alpha})$  yield the same data distribution and therefore cannot be distinguished from each other. But generically, this translation-rotation ambiguity is the only source of non-identifiability, shown by Proposition 1 below.

**PROPOSITION 1.** *Assume  $n > 2(k + 2)$ . Then there exists a set  $\mathcal{N} \subset \mathbb{R}^{n \times (k+1)}$  with zero Lebesgue measure such that, for any  $[Z^*, \alpha^*]$  and  $[\tilde{Z}, \tilde{\alpha}] \notin \mathcal{N}$  satisfying  $\text{vech}(\Theta^*) = \text{vech}(\tilde{\Theta})$ , there exist  $Q \in \mathcal{O}(k)$  and  $c \in \mathbb{R}^k$  such that (2) holds.*

If self-loops  $A_{ii}$  are observed and also follow (1), i.e.,  $A_{ii} \sim p(\cdot | \Theta_{ii})$ , then the same identifiability holds without the need to exclude a zero-measure set. Proposition 1 considers a more challenging scenario where the diagonal  $\Theta_{ii}$  information is unavailable, and therefore only generic identifiability can be established, which is consistent with the existing literature [5]. We focus on the no-self-loops scenario, since meaningful self-loops are often unavailable in real-world datasets, and the corresponding theoretical developments need to address additional technical caveats. More details are discussed in Section C of the Supplementary Material. Proposition 1 implies that true parameters yielding the same distribution form an equivalence class. To simplify the presentation, we introduce the following regularity conditions on  $(Z^*, \alpha^*)$ , which will specify a convenient representative in the equivalence class.

**CONDITION 1 (True parameters).** Assume  $(Z^*, \alpha^*)$  satisfy:

- (i)  $1_n^\top Z^* = 0$  and  $Z^{*\top} Z^*$  is diagonal.
- (ii) There exists a positive constant  $M_1$  such that  $\|Z^*\|_{2 \rightarrow \infty} \leq M_1$  and  $\|\alpha^*\|_\infty \leq M_1$ .
- (iii) There exists a positive constant  $M_2$  such that  $\sigma_{\min}[Z^{*\top} Z^*/n] \geq M_2$ , where  $\sigma_{\min}(\cdot)$  represents the minimum singular value of the input matrix.

Condition 1 is comparable to Assumptions II–IV in Li et al. [19], except that we do not require that the limit of  $Z^{*\top} Z^*/n$  has unique eigenvalues. In Condition 1 (i), the constraint  $1_n^\top Z^* = 0$  fixes the translational indeterminacy by centering the latent vectors, while the diagonality of  $Z^{*\top} Z^*$  specifies a particular coordinate system for the latent space. These two constraints can be imposed without loss of generality, since the model is invariant to translations and rotations of the latent vectors by Proposition 1. Specifically, given any  $(Z^*, \alpha^*)$ , we can construct  $(\tilde{Z}, \tilde{\alpha})$  following (2) with  $c^\top = 1_n^\top Z^*/n$  and  $Q$  being an orthogonal matrix formed by right singular vectors of  $Z^* - 1_n c^\top$ . Then  $(\tilde{Z}, \tilde{\alpha})$  satisfies Condition 1 (i) and yields the same data distribution as  $(Z^*, \alpha^*)$  does. When  $Z^* - 1_n c^\top$  has repeated singular values, the choice of  $Q$  is not unique, but any choice gives an equivalent representative. Moreover, Condition 1 (ii)–(iii) assume the parameters are bounded and  $Z^{*\top} Z^*/n$  is well-conditioned. These assumptions are common and standard in the related literature [14, 22, 48, 49] and can facilitate theoretical analysis.

### 3. Gaps Between Existing Theory and Practice.

**3.1. Constrained Maximum Likelihood Estimator.** Under the latent space model (1), Li et al. [19] establish the asymptotic distribution of the maximum likelihood estimator under constraints. In particular, they consider maximizing the log likelihood function  $\sum_{1 \leq i < j \leq n} \ell(\Theta_{ij}; A_{ij})$  with  $\ell(\theta; x) = \log p(x | \theta)$  and  $\Theta_{ij} = \alpha_i + \alpha_j + \langle z_i, z_j \rangle$  under the constraints

$$(3) \quad \|Z\|_{2 \rightarrow \infty} \leq M, \quad \|\alpha\|_\infty \leq M, \quad 1_n^\top Z = 0, \quad \text{and } Z^\top Z \text{ is diagonal.}$$

The first two inequalities in (3) constrain the parameters to be bounded. The zero-mean constraint on  $Z$  removes the translational non-identifiability as described in (2). Further restricting  $Z^\top Z$  to be diagonal sets a particular coordinate system for the latent space, under which  $Z$  is identifiable up to sign flip when  $Z^\top Z/n$  has distinct eigenvalues. More technical explanations are provided in Section 4.1.

Classical inferential theory is not directly applicable to analyze the log likelihood under the latent space model, because the likelihood function is non-convex in  $[Z, \alpha]$ , and the number of parameters grows with respect to the network size  $n$  at an unconventional rate (see Remark 1 for more details). To address these difficulties, [19] propose augmenting the likelihood with a Lagrange multiplier penalty proportional to

$$(4) \quad \|\text{vech}(Z^\top Z)\|_2^2 + \|Z^\top \mathbf{1}_n\|_2^2,$$

which is motivated from constraints in (3). Then [19] show the Lagrange-adjusted likelihood function is strongly convex with high probability, thereby facilitating the proofs. More broadly, auxiliary Lagrange multiplier terms have long been used in constrained maximum likelihood estimation and in likelihood analyses with singular information matrices, dating back to [1] and [10] in low-dimensional problems. Wang [44] extends a related idea to high-dimensional generalized factor models. Although the augmenting idea is shared, different model properties induce distinct technical challenges. Under the latent space networks, [19] further tackle with unique symmetric formulations and carefully control residual errors with the specific penalty in (4).

Despite these advances for network models, the theoretical analysis in [19] has several limitations from a practical perspective. First, their asymptotic theory requires  $Z^{*\top} Z^*/n$  to converge to a diagonal matrix with distinct eigenvalues, while additional constraints are needed to handle repeated eigenvalues. Such a case-specific treatment could be unsatisfactory in practice, where prior spectral information is often unavailable, necessitating a unified approach that accommodates various scenarios. Second, the upper bound  $M$  in (3) is required to be sufficiently large so that the underlying true parameters  $[Z^*, \alpha^*]$  fall within the feasible regime. Since true parameters are typically unknown in practice, the implications of this constraint on practical usage and interpretation remain ambiguous. Third, [19] exclusively analyzes the constrained maximum likelihood estimator, whereas its relationship to the actual outputs of practical algorithms is unclear.

**REMARK 1 (Challenges in classical analysis).** To make this paper self-contained, we briefly describe the technical difficulties that are also mentioned in [19]. For the simplicity of notation, let  $y \in \mathbb{R}^{n(k+1)}$  denote the vectorization of  $[Z, \alpha]$ , and let  $L(y)$  denote the negative log likelihood function, with its gradient denoted as  $S_L(y)$ . The classical route to deriving the distribution of a maximum likelihood estimator utilizes the first-order optimality condition and the Taylor expansion [42]. In our problem, that is,  $0 = S_L(\hat{y}) = S_L(y^*) + H_L(y^*)(\hat{y} - y^*) + R(\hat{y}, y^*)$ , where  $R(\hat{y}, y^*)$  denotes the residual term. If  $R(\hat{y}, y^*)$  is uniformly small and the Hessian matrix  $H_L(y^*)$  is invertible, one might obtain  $\hat{y} - y^* = -\{H_L(y^*)\}^{-1} S_L(y^*) +$  small-order residuals, serving as a starting point for deriving asymptotic distributions of the entries in  $\hat{y} - y^*$  in canonical settings. However, the leading term in  $H_L(y^*)$  turns out to have exactly  $k(k+1)/2$  zero eigenvalues, and the dimension of  $y$ , namely  $n(k+1)$ , is large compared to the effective sample size  $n(n-1)/2$ , making it difficult to apply the standard argument. More details on the characterization of the null space of  $H_L(y^*)$  are provided in Remark B.5 in the Supplementary Material.

**3.2. Projected Gradient Descent and Universal Singular Value Thresholding.** Practically, to compute the constrained maximum likelihood estimator, [19] adopt a common strategy in the existing literature: a singular value thresholding procedure as in Algorithm 3 of

[22] and a projected gradient descent method as in Algorithm 1 of [22] for initialization and optimization, respectively. Such a two-stage approach has been widely used and generalized in various network models [14, 40, 49].

The projected gradient descent method (Algorithm 1 in [22]) estimates the latent vectors under a non-convex optimization framework. This approach iteratively updates  $Z$  and  $\alpha$  parameters along their gradient directions and then projects the updates onto a feasible regime like (3) to enforce boundedness and the centering constraint. Ma, Ma and Yuan [22] establish the convergence of the algorithmic output to the true latent parameters under the Frobenius norm. However, their analysis has two key limitations when integrated with the inferential results in [19]. First, [22] evaluate the discrepancy between the algorithmic output and the true parameters  $[Z^*, \alpha^*]$ , which essentially conflates both algorithmic convergence error and the irreducible statistical error. To apply the inferential results of [19] in practice, these two sources of errors need to be properly decoupled, necessitating a more refined analysis. Second, the theoretical arguments in [22] require hyperparameters to be chosen in a way relying on the unknown true parameters, such as the boundedness set in the projection step and the learning rate in the projected gradient descent. These requirements are often impractical and limit the developments of reliable and fully data-driven inference.

In addition, the initialization procedure in Algorithm 3 of [22] is built on the universal singular value thresholding (USVT) method introduced by Chatterjee [8]. Both [22] and [8] consider bounded entries in adjacency matrices, such as binary edges in networks. Moreover, [22] suggest a projection step to regularize the range of estimates, similarly to the projected gradient descent. However, when the true parameters are unknown, it is unclear how to choose the projection set in a principled way without prior knowledge of the true parameters under general data distributions.

To address the above issues in the existing literature, we develop a comprehensive analysis of both the maximum likelihood estimator and the practical estimation procedure, covering the USVT-based initialization and the projected gradient descent algorithm. These contributions are detailed in Sections 4 and 5, respectively.

**4. Maximum Likelihood Estimator with Flexible Eigenvalue Multiplicity.** In this section, we examine the constrained maximum likelihood estimator and its asymptotic theory without imposing the unique-eigenvalue assumption on  $Z^{*\top} Z^*/n$  used in [19]. Specifically, we let  $(\hat{Z}, \hat{\alpha})$  be one of the solution that maximizes the log likelihood function, or equivalently, any solution to the following optimization problem

$$(5) \quad \begin{aligned} \arg \min_{Z \in \mathbb{R}^{n \times k}, \alpha \in \mathbb{R}^n} \quad & L(Z, \alpha) := - \sum_{1 \leq i < j \leq n} \ell(\Theta_{ij}; A_{ij}) \\ \text{subject to} \quad & \|Z\|_{2 \rightarrow \infty} \leq M, \|\alpha\|_{\infty} \leq M, \mathbf{1}_n^\top Z = 0. \end{aligned}$$

Different from the constraints in (3) imposed by [19], (5) does not require  $Z^\top Z$  to be diagonal and thus is more flexible in practice. Nevertheless, their proposed Lagrange multiplier (4) cannot be used, necessitating new developments in theoretical analysis.

*4.1. Implicit regularization from orthogonal Procrustes problem.* We begin by explaining a fundamental limitation in the existing analysis, which in turn motivates our new strategy. As reviewed in Section 3.1, [19] address the non-identifiability of  $Z$  by restricting  $\mathbf{1}_n^\top Z = 0$  and  $Z^\top Z$  to be diagonal, which are intended to resolve the ambiguities from arbitrary mean shift and  $\mathcal{O}(k)$  transformation, respectively. Although the centering constraint effectively removes the mean-shift ambiguity, the diagonality restriction does not fully resolve the non-identifiability from  $\mathcal{O}(k)$  transformations.

To see this, consider two candidate matrices  $[Z^*, \alpha^*]$  and  $[\tilde{Z}, \tilde{\alpha}] \in \mathbb{R}^{n \times (k+1)}$  satisfying  $1_n^\top Z^* = 1_n^\top \tilde{Z} = 0$  and both yield the same likelihood. By Proposition 1, we know (2) holds up to a zero measure set. The centering constraint forces  $c = 0$ , so there exists  $Q \in \mathcal{O}(k)$  such that  $\tilde{Z}Q = Z^*$ . Now further assume both  $Z^{*\top} Z^*$  and  $\tilde{Z}^\top \tilde{Z}$  are diagonal with diagonal entries in non-increasing order. If both have unique eigenvalues,  $Q$  must equal a signature matrix  $\text{diag}(q_1, \dots, q_k)$  for  $q_i \in \{-1, +1\}$ , implying that columns of  $Z$  and  $\tilde{Z}$  can be matched up to sign flips. In contrast, if  $Z^{*\top} Z^*$  and  $\tilde{Z}^\top \tilde{Z}$  are proportional to the identity matrix, then their eigenvalues are repeated, and  $Q \in \mathcal{O}(k)$  is not necessarily diagonal. As a result, there is no clear one-to-one correspondence between the columns of  $Z^*$  and  $\tilde{Z}$ . More generally, when only a subset of eigenvalues of  $Z^{*\top} Z^*$  (or  $\tilde{Z}^\top \tilde{Z}$ ) are repeated, only the columns associated with distinct eigenvalues are identifiable up to sign, whereas the remaining columns are not.

The preceding discussion shows that directly examining the algebraic difference between two latent-vector matrices would inevitably require additional restrictions and cumbersome case-by-case discussions, thereby obscuring the practical implications. Instead, to obtain a unified characterization without unnecessary restrictions on the spectrum of  $Z^*$ , it is more natural to measure discrepancy only up to the best orthogonal transformation in  $\mathcal{O}(k)$ . In particular, given any minimizer  $(\hat{Z}, \hat{\alpha})$  of the constrained optimization problem (5), define

$$(6) \quad \hat{Z}_q = \hat{Z} \hat{Q}^\top, \quad \text{with } \hat{Q} = \arg \min_{Q \in \mathcal{O}(k)} \|\hat{Z} - Z^* Q\|_F.$$

We propose to examine  $\hat{Z}_q - Z^* = \hat{Z} \hat{Q}^\top - Z^*$  and establish asymptotic distributions of its entries. Since  $\hat{Z}_q$  differs from  $\hat{Z}$  only by  $\hat{Q} \in \mathcal{O}(k)$ , they yield the identical likelihood by the arguments in Section 2 and hence give the same statistical interpretation. Meanwhile, the aligned difference  $\hat{Z}_q - Z^*$  removes ambiguities from sign flips or repeated eigenvalues, so it resolves the non-identifiability from  $\mathcal{O}(k)$  transformations fundamentally. Conceptually, this formulation eliminates the need to assume unique limiting eigenvalues of  $Z^{*\top} Z^*/n$  in theory. Further technical discussions are provided in Remark 2 below.

Technically, without restricting the diagonality of  $Z^\top Z$ , it may appear that the non-convexity issue discussed in Section 3.1 still persists. But interestingly, the best  $\mathcal{O}(k)$  alignment induces an implicit regularization in the sense that for any two matrices  $\hat{Z}$  and  $Z^* \in \mathbb{R}^{n \times k}$ ,  $\hat{Z}_q$  defined in (6) always satisfies

$$(7) \quad \hat{Z}_q^\top Z^* = Z^{*\top} \hat{Z}_q.$$

This identity follows from classical results on the orthogonal Procrustes problem and is originally shown in [39]. Thus, when studying latent vectors up to the best  $\mathcal{O}(k)$  alignment, one can impose an extra constraint (7) without loss of generality, which addresses the non-identifiability in a more natural way. In the proof, we introduce a new Lagrange multiplier penalty  $P^*(Z) := \|\text{vech}(Z^\top Z^* - Z^{*\top} Z)\|_2^2 + \|Z^\top 1_n\|_2^2$ , corresponding to two sets of constraints  $Z^\top Z^* = Z^{*\top} Z$  and  $Z^\top 1_n = 0$  to address the ambiguity from  $\mathcal{O}(k)$  transformation and mean shift, respectively. Our proof shows that the Hessian matrix of  $L(Z, \alpha) + P^*(Z)$  is non-singular with high probability, thereby overcoming the non-convexity challenge explained in Remark 1. We defer further technical explanations to Remark 3 below.

The proposed implicit constraints and the augmenting penalty have several notable features. First, the penalty  $P^*(Z)$  relies on unknown true parameter  $Z^*$  and is neither computable nor usable in practice. It only serves as an intermediate technical device, rather than a practical regularization term such as the lasso or ridge penalty. Second, by the construction, the constraints  $Z^\top Z^* = Z^{*\top} Z$  and  $Z^\top 1_n = 0$  contribute a total of  $k(k+1)/2$  number of constraints, which coincides with the dimension of the intrinsic null space of the Hessian matrix of  $L(Z, \alpha)$  mentioned in Remark 1. Third, even when  $Z^{*\top} Z^*/n$  has repeated limiting eigenvalues, we show that the leading term in the Hessian matrix of  $L(Z, \alpha) + P^*(Z)$

is still non-singular with high probability. In contrast, using the augmenting penalty in [19], i.e., replacing  $P^*(Z)$  by (4), the corresponding leading term has exactly zero eigenvalues. Details are provided in Remark B.5 of the Supplementary Material.

**REMARK 2 (Uniqueness of  $\hat{Z}_q - Z^*$ ).** First, given two fixed matrices  $\hat{Z}$  and  $Z^* \in \mathbb{R}^{n \times k}$ ,  $\hat{Q} = UV^\top$  with  $U\Sigma V^\top$  denoting the singular value decomposition of  $Z^{*\top}\hat{Z}$  is always one of the solutions to  $\min_{Q \in \mathcal{O}(k)} \|\hat{Z} - Z^*Q\|_F$  [12]. This minimizer is unique if  $Z^{*\top}\hat{Z}$  is non-singular. We next focus on this regime, because we show  $Z^{*\top}\hat{Z}$  is non-singular with high probability in the proof of Theorem 1 (see Remark D.1 in the Supplementary Material). Then we can interpret  $\hat{Q}$  as the orthogonal transformation that best aligns  $Z^*$  with  $\hat{Z}$ , and symmetrically,  $\hat{Q}^\top$  best aligns  $\hat{Z}$  with  $Z^*$  in the sense that  $\hat{Q}^\top = \arg \min_{Q \in \mathcal{O}(k)} \|\hat{Z}Q - Z^*\|_F$ . Second, the aligned difference  $\hat{Z}_q - Z^*$  remains unchanged if replacing  $\hat{Z}$  with  $\hat{Z}\tilde{Q}$  for any  $\tilde{Q} \in \mathcal{O}(k)$  when  $Z^{*\top}\hat{Z}$  is non-singular. Therefore, in such a non-singular regime relevant to our analysis,  $\hat{Z}_q - Z^*$  is a well-defined quantity to examine the difference between a fixed  $Z^*$  and the equivalence class of  $\hat{Z}$  with respect to  $\mathcal{O}(k)$  transformations.

**REMARK 3 (Details for score augmentation).** To shed light on theoretical derivations, we provide a sketch on how we address the non-convexity issue highlighted in Remark 1 via score augmentation. Let  $y$  denote the vectorization of  $[Z, \alpha]$  like in Remark 1, and define  $P^*(y) = P^*(Z)$  with its gradient denoted as  $S_{P^*}(y)$ . Our argument consists of three parts. First, we show  $S_L(\hat{y}) = 0$  if and only if  $S_L(\hat{y}_q) = 0$  where  $\hat{y}_q$  denotes the vectorization of  $[\hat{Z}_q, \hat{\alpha}]$  defined in (6). Second, we argue  $S_{P^*}(\hat{y}_q) = 0$  based on the implicit regularization (7). Third, the first-order condition  $S_L(\hat{y}) = 0$  in Remark 1 can therefore be equivalently reformulated as the augmented score equation  $S_L(\hat{y}_q) + S_{P^*}(\hat{y}_q) = 0$ . We will then show that the augmented score has a non-singular Hessian matrix  $H(y^*)$  with high probability, without imposing restrictions on the spectrum of  $Z^{*\top}Z^*$ . Heuristically, this enables an expansion  $\hat{y}_q - y^* = -\{H(y^*)\}^{-1}S_L(y^*) + \text{small-order residuals}$  to examine the asymptotic distribution of  $\hat{Z}_q - Z^*$  and  $\hat{\alpha} - \alpha^*$ . Although this score expansion is motivated from classical maximum likelihood theory, our problem has specific properties that pose unique technical difficulties. For example, the first-order condition is not directly available due to the constraints in (5), the Hessian matrix has a special structure, and the residual terms are high-dimensional. Our proof carefully overcomes all the technical issues arising from our unique problem properties. Notably, our analysis applies to any solution of (5) without the need to diagonalize  $\hat{Z}^\top\hat{Z}$ , and thus differs significantly from [19].

**4.2. Asymptotic Theory for Constrained Maximum Likelihood Estimator.** We next develop asymptotic theory for the constraint-relaxed estimator in (5). For the formal theoretical developments, we impose the following regularity condition on the edgewise distribution.

**CONDITION 2 (Edgewise distributions).** Let  $\mathcal{X} = \{x \in \mathbb{R} : p(x | \theta) > 0\}$  denote the support of  $p(x | \theta)$ . Assume  $\ell(\theta; x) = \log p(x | \theta)$  in (1) satisfies the following conditions.

- (i) For any fixed  $x \in \mathcal{X}$ ,  $\ell(\theta; x)$  is three times differentiable with respect to  $\theta$ , with its first to third derivatives with respect to  $\theta$  denoted by  $\ell'(\theta; x)$ ,  $\ell''(\theta; x)$ , and  $\ell'''(\theta; x)$ , respectively. Moreover, for any constant  $b > 0$ , there exist constants  $\kappa_1(b), \kappa_2(b), \kappa_3(b) > 0$  such that

$$\kappa_1(b) \leq -\ell''(\theta; x) \leq \kappa_2(b) \quad \text{and} \quad |\ell'''(\theta; x)| \leq \kappa_3(b) \quad \text{for all } \theta \in [-b, b] \text{ and } x \in \mathcal{X}.$$

- (ii) There exist constants  $K, s > 0$  such that for any  $t \geq 0$ ,  $\Pr(|\ell'(\Theta_{ij}^*; A_{ij})| > t) \leq 2 \exp(-(t/K)^s)$ .

Condition 2 is similar to Assumptions V and VI in Li et al. [19]. First, Condition 2 (i) implies that  $\ell(\theta, x)$  is concave and its derivatives remain bounded when  $\theta$  belongs to a bounded regime. This can be satisfied by common exponential family distributions, such as standard normal, Bernoulli, and Poisson distribution with canonical link functions. Second, Condition 2 (ii) implies that the edgewise score function follows a sub-Weibull tail distribution, which generalizes the common sub-gaussian and sub-exponential tail properties [17, 43]. In addition, a common edgewise distribution family  $\ell(\theta; x)$  is considered just for notational simplicity, and all the conclusions can be similarly generalized by allowing the distributional types of  $A_{ij}$  to vary across  $1 \leq i < j \leq n$ .

REMARK 4 (Existence of the constrained MLE). The constrained MLE defined in (5) always exists under our assumptions. In particular, the objective function  $L(Z, \alpha)$  in (5) is continuously differentiable with respect to  $[Z, \alpha]$  by Condition 2 (i), and the feasible set in (5) is compact by its formulation. Hence, by the Weierstrass extreme value theorem,  $L(Z, \alpha)$  attains its minimum over the compact feasible set, so the defined minimizer  $\hat{Y}$  exists.

To facilitate the presentation, we concatenate  $z_i$  and  $\alpha_i$  for each node  $1 \leq i \leq n$  as

$$(8) \quad y_i = \begin{bmatrix} z_i \\ \alpha_i \end{bmatrix} \in \mathbb{R}^{k+1}, \quad \text{and define} \quad \Sigma_i(Y) = - \sum_{j=1}^n \ell''(\Theta_{ij}; A_{ij}) w_j w_j^\top \in \mathbb{R}^{(k+1) \times (k+1)},$$

where  $w_j = \partial \Theta_{ij} / \partial y_i = [z_j^\top, 1]^\top \in \mathbb{R}^{k+1}$ , and  $Y = [y_1, \dots, y_n]^\top = [Z, \alpha] \in \mathbb{R}^{n \times (k+1)}$ . Given a set of  $m$  node indices  $\mathcal{I} = (i_1, \dots, i_m)$ , we denote the concatenated vector

$$(9) \quad y_{\mathcal{I}} = \begin{bmatrix} y_{i_1} \\ \vdots \\ y_{i_m} \end{bmatrix} \in \mathbb{R}^{m(k+1)} \quad \text{and} \quad \Sigma_{\mathcal{I}}(Y) = \begin{bmatrix} \Sigma_{i_1} & \cdots & 0 \\ \vdots & \ddots & \vdots \\ 0 & \cdots & \Sigma_{i_m} \end{bmatrix} \in \mathbb{R}^{m(k+1) \times m(k+1)}$$

being a block-diagonal matrix. For the maximum likelihood estimator, we let  $\hat{Y}_q = [\hat{Z}_q, \hat{\alpha}]$  with  $\hat{Z}_q$  in (6) and define  $\hat{y}_{q, \mathcal{I}}$  and  $\Sigma_{\mathcal{I}}(\hat{Y}_q)$  similarly to (9) with  $Y$  replaced by  $\hat{Y}_q$ . We next state the main asymptotic result.

THEOREM 1. Assume Conditions 1–2, and the constant  $M$  in (5) satisfies

$$(10) \quad M \geq 2M_1 \quad \text{with } M_1 \text{ in Condition 1.}$$

- (i) For any constant  $\varepsilon > 0$ , there exist constants  $C_\varepsilon > 0$  and  $N_\varepsilon \in \mathbb{N}$  such that when  $n \geq N_\varepsilon$ , with probability  $1 - O(n^{-\varepsilon})$ ,  $\hat{\alpha}$  is unique and  $\hat{Z}$  is unique up to the orthogonal group  $\mathcal{O}(k)$ , and

$$\|\hat{Y}_q - Y^*\|_{2 \rightarrow \infty} \leq C_\varepsilon n^{-1/2} \log(n).$$

- (ii) For any fixed index set  $\mathcal{I}$  of  $m$  nodes, as  $n$  goes to infinity,

$$\{\Sigma_{\mathcal{I}}(\hat{Y}_q)\}^{1/2} (\hat{y}_{q, \mathcal{I}} - y_{\mathcal{I}}^*) \xrightarrow{d} \mathcal{N}(0, \mathbf{I}_{m(k+1)}).$$

Theorem 1 first establishes the uniqueness of the constrained maximum likelihood estimator  $\hat{Y} = [\hat{Z}, \hat{\alpha}]$  up to  $\mathcal{O}(k)$  transformations. Although  $\hat{Z}$  is not strictly unique as a matrix, it can be naturally interpreted as an equivalent class up to  $\mathcal{O}(k)$ . The aligned estimator  $\hat{Y}_q = [\hat{Z}_q, \hat{\alpha}]$  serves as a convenient canonical representative for inference. The unknown orthogonal matrix  $\hat{Q}$  merely determines the coordinate system for representing the latent space and does not hinder statistical interpretation for the intrinsic discrepancy. Second, the

two-to-infinity error bound suggests the maximum likelihood estimator achieves uniform consistency across all parameters as  $n \rightarrow \infty$ . Third, Theorem 1 further establishes entrywise asymptotic normality of the aligned estimator  $\hat{Y}_q$ . When  $p(\cdot | \theta)$  follows a natural exponential family distribution with canonical link function, we actually have that  $\Sigma_i$  equals the Fisher information matrix of  $y_i = [z_i^\top, \alpha_i]^\top$ , that is,  $\Sigma_i = \mathbb{E}(\frac{\partial L}{\partial y_i} \frac{\partial L}{\partial y_i}^\top)$ .

Although the conclusions in Theorem 1 resemble that in [19], the scope here is broader without enforcing  $\hat{Z}^\top \hat{Z}$  to be diagonal or  $Z^{*\top} Z^*$  to have distinct limiting eigenvalues. Therefore, Theorem 1 provides a unified inferential result showing that the same asymptotic structure remains valid regardless of eigenvalue multiplicity. This broadens the applicability of the inferential theory and paves the way for connecting to practical algorithms under more flexible and realistic constraints, which will be discussed in Section 5.

**REMARK 5 (Invariance with respect to  $M$ ).** Interestingly, our proof reveals that the constrained MLE defined in (5) is invariant to the choice of  $M$ , provided  $M$  is sufficiently large as required in (10). In other words, any two values of  $M$  satisfying (10) yield identical solutions in (5) with high probability. This is formally justified in Remark D.2 of the Supplementary Material. Therefore,  $\hat{Y}$  is well-defined without requiring a uniquely specified  $M$ . This invariance is also reflected in the practical algorithm in Section 5, where the empirical estimator approximates  $\hat{Y}$  in (5) without explicitly specifying  $M$ .

The asymptotic results in Theorem 1 provide a foundation for various downstream inferential tasks, where the target of interest is a transformation of  $Y^* = [Z^*, \alpha^*]$ . For example, for any pair of nodes  $(i, j)$ , their corresponding edgewise mean is

$$(11) \quad \mathbb{E}(A_{ij} | \Theta^*) = \mu(\Theta_{ij}^*) = \mu(\langle z_i^*, z_j^* \rangle + \alpha_i^* + \alpha_j^*),$$

where  $\mu(\cdot)$  denotes the link function between the expectation and parameters under the distribution  $p(\cdot | \theta)$  in (1). More generally, let  $g(\cdot)$  be a fixed function of  $y_{\mathcal{I}} \in \mathbb{R}^{m(k+1)}$ , where  $\mathcal{I}$  is a fixed index set as in Theorem 1. By Theorem 1, the induced maximum likelihood estimator of  $g(y_{\mathcal{I}}^*)$  is  $g(\hat{y}_{q,\mathcal{I}})$ , and we next establish its asymptotic distribution.

**COROLLARY 1.** *For a given fixed index set  $\mathcal{I}$  of  $m$  nodes, define  $y_{\mathcal{I}}^*$  and  $\hat{y}_{q,\mathcal{I}}$  as in Theorem 1. Let  $g: \mathbb{R}^{m(k+1)} \rightarrow \mathbb{R}$  be a fixed function that is twice continuously differentiable, and denote its gradient by  $\nabla g(\cdot)$ . Assume the conditions of Theorem 1, and the regularity condition on  $g(\cdot)$  stated in Condition E.1 in the Supplementary Material. Then, as  $n \rightarrow \infty$ ,  $\{g(\hat{y}_{q,\mathcal{I}}) - g(y_{\mathcal{I}}^*)\} / \widehat{se}(\hat{g}_{\mathcal{I}}) \xrightarrow{d} \mathcal{N}(0, 1)$ , where we denote*

$$\widehat{se}(\hat{g}_{\mathcal{I}}) := \left\{ \nabla g(\hat{y}_{q,\mathcal{I}})^\top \Sigma_{\mathcal{I}}(\hat{Y}_q)^{-1} \nabla g(\hat{y}_{q,\mathcal{I}}) \right\}^{1/2}.$$

As an illustration, consider inference for the edgewise mean in (11) by Corollary 1. Construct  $\hat{\Theta}_{ij} := \langle \hat{z}_{q,i}, \hat{z}_{q,j} \rangle + \hat{\alpha}_i + \hat{\alpha}_j = \langle \hat{z}_i, \hat{z}_j \rangle + \hat{\alpha}_i + \hat{\alpha}_j$ . By Corollary 1 and the chain rule, we have  $\{\mu(\hat{\Theta}_{ij}) - \mu(\Theta_{ij}^*)\} / \widehat{se}(\hat{\mu}_{ij}) \xrightarrow{d} \mathcal{N}(0, 1)$  under suitable conditions, where

$$(12) \quad \widehat{se}(\hat{\mu}_{ij}) := \left| \mu'(\hat{\Theta}_{ij}) \right| \left\{ \begin{bmatrix} \hat{w}_j \\ \hat{w}_i \end{bmatrix}^\top \begin{bmatrix} [\Sigma_i(\hat{Y})]^{-1} & 0 \\ 0 & [\Sigma_j(\hat{Y})]^{-1} \end{bmatrix} \begin{bmatrix} \hat{w}_j \\ \hat{w}_i \end{bmatrix} \right\}^{1/2},$$

and  $\mu'(\cdot)$  denotes the derivative of  $\mu(\cdot)$ .

**5. Adaptive Algorithms and Theoretical Guarantees.** In this section, we develop a fully data-adaptive computational framework whose output converges to the maximum likelihood estimator  $[\hat{Z}, \hat{\alpha}]$  with high probability. In particular, Sections 5.1–5.3 study the adaptive projected gradient descent, covering the algorithm, its convergence theory, and additional implementation details, respectively. Sections 5.4–5.5 then develop a range-adaptive singular value thresholding for initialization along with theoretical guarantees.

5.1. *Projected Gradient Descent Algorithm with Adaptive Learning Rate.* As reviewed in Section 3, solving the MLE (5) is typically achieved by the projected gradient descent algorithm [22]. However, bridging the algorithm output in practice and the idealized MLE (5) is faced with several challenges. First, the objective function is non-convex and the dimension of parameters is high. Second, Theorem 1 suggests that the solution in (5) is relevant to inferring true parameters  $Y^*$  if  $M \geq 2M_1$ , but in practice  $M_1$  is unknown. Therefore, it can be unclear how  $M$  should be chosen. Third, existing analyses in [22] require certain tuning parameters to be chosen in a way relying on unknown model truth, such as the learning rate and projection set, and therefore become impractical.

To address all these challenges, we devise a novel backtracking line search scheme that produces data-adaptive learning rates and develop new proof techniques showing that the explicit projection onto an unknown set can be avoided. A pseudo-code summary of the proposed algorithm is given in Algorithm 1, and we now explain the details. Overall, Algorithm 1 takes iterates over projected gradient descent, and each iteration consists of three major stages. The first stage computes the search direction

$$(13) \quad d(Y) = -[J_n \nabla_Z L(Y), \nabla_\alpha L(Y)],$$

where  $J_n = I_n - 1_n 1_n^\top / n$ , and  $\nabla_Z L(Y)$  and  $\nabla_\alpha L(Y)$  represent partial derivatives of  $L(Y) = L(Z, \alpha)$  with respect to  $Z$  and  $\alpha$ , respectively. Note that  $d(Y)$  differs from the gradient descent direction  $-\nabla_Y L(Y)$  only by a projection matrix  $J_n$  multiplied to  $\nabla_Z L(Y)$ . As  $1_n^\top J_n = 0$ , multiplying  $J_n$  ensures that the updates to  $Z$  part are centered, so that updated latent vectors from each iteration satisfy the identifiability constraint  $1_n^\top Z = 0$ . The second stage runs a line search to adaptively determine an appropriate learning rate  $\eta$ . Due to the non-convexity and high dimensionality of the optimization problem in (5), classical line search methods and analyses used in convex optimization cannot directly yield convergence guarantee. To address that, we introduce a novel set of search rules. Specifically, given a current iterate  $Y$  (for example,  $Y = Y^r$  for  $Y^r$  estimate in the  $r$ -th iteration), a candidate step size  $\eta$  is accepted if the following conditions are simultaneously satisfied

$$(14) \quad L(Y + \eta d(Y)) - L(Y) - C_{\text{ls}} n \eta^2 \langle \nabla_Y L(Y), d(Y) \rangle \leq 0,$$

$$(15) \quad \text{and } \max_{1 \leq i \leq n} \{L_i(Y + \eta d_i(Y)) - L_i(Y) - C_{\text{ls}} n \eta^2 \langle \nabla_Y L_i(Y), d_i(Y) \rangle\} \leq 0,$$

where we define  $d_i(Y) = -e_i e_i^\top \nabla_Y L(Y)$ ,  $e_i$  is an  $n$ -dimensional indicator vector with only the  $i$ -th position being one and zero otherwise, and  $L_i = -\sum_{j \in \{1, \dots, n\} \setminus \{i\}} \ell(\Theta_{ij}; A_{ij})$ , and  $C_{\text{ls}}$  is a hyperparameter that can be simply set to 1 in our framework. Similarly to classical backtracking line search [28], we start with an initial value of  $\eta$  and iteratively shrink it by a contraction factor  $\beta \in (0, 1)$  until both (14) and (15) are satisfied. In practice, one may also set a limit for the number of shrinking iterations to prevent pathological cases. Finally, the third stage updates the parameters along the descent direction with the selected learning rate.

We next discuss connections and differences between the proposed search rules (14)–(15) and existing methods in the literature. First, (14) takes a form similar to the classical Armijo condition in convex optimization; see Remark 6 for a description. However, (14) specifies a factor  $n\eta^2$  before the cross product term  $\langle \nabla_Y L(Y), d(Y) \rangle$  which is quadratic in  $\eta$  rather than linear as in the classical Armijo condition. This modification is crucial for addressing the theoretical challenges from intrinsic non-convexity and high-dimensionality of our problem. Second, (15) is equivalent to imposing  $n$  conditions on  $L_i(Y)$  and  $d_i(Y)$  with  $i \in \{1, \dots, n\}$  simultaneously. For each  $i = 1, \dots, n$ , the inequality constraint takes a form similar to (14). But  $Y + \eta d_i(Y)$  differs from  $Y$  only by updating its  $i$ -th row  $y_i$  along the direction  $-\nabla_{y_i} L(Y)$ . Intuitively, (15) evaluates the “goodness” of update along each row of  $Y$ , whereas (14) evaluates the update of the whole matrix  $Y$ . Technically, imposing

---

**Algorithm 1:** Projected Gradient Descent with Adaptive Line Search.
 

---

**Input:** Data:  $A \in \mathbb{R}^{n \times n}$ . Initial estimate:  $Y^0 \in \mathbb{R}^{n \times (k+1)}$ . Initial step size:  $\eta_{\text{init}} > 0$ .  
 Backtracking rate and steps:  $\beta \in (0, 1)$  and  $R' \in \mathbb{N}$ . Number of iterations:  $R$ .

```

1 for  $r = 0, \dots, R - 1$  do
2   I. Compute descent direction.    $d(Y^r) = -[J_n \nabla_Z L(Y^r), \nabla_\alpha L(Y^r)]$ .
3   II. Line search.
4     Initialize  $\eta = \eta_{\text{init}}$ ;
5     if (14) or (15) is violated with  $Y = Y^r$  and the current  $\eta$  then
6       repeat
7          $\eta = \beta \eta$ 
8       until (14) and (15) both hold, or the number of backtracking exceeds  $R'$ ;
9     end
10    return final step size for the  $r$ -th iteration:  $\eta_r = \eta$ .
11  III. Update.    $Y^{r+1} = Y^r + \eta_r d(Y^r)$ .
12 end

```

**Output:**  $Y^R$ .

---

(15) ensures row-wise control needed in the convergence analysis. This helps overcome the necessity of projecting onto an unknown set in the original Algorithm 1 in [22]. Notably, both (14) and (15) are data-adaptive and practically flexible.

**REMARK 6 (Classical Armijo condition).** For comparison, we give a simple example of minimizing a convex function  $f(x)$  with  $x \in \mathbb{R}^k$  by the line search method under the classical Armijo condition [28]. At the  $r$ -th iteration, let  $x_r$  denote the estimate for the current iterate and let  $d_r$  be a descent direction satisfying  $\langle \nabla f(x_r), d_r \rangle < 0$ . By iteratively shrinking from an initially large  $\eta$ , classical Armijo condition accepts the first value of  $\eta$  that satisfies  $f(x_r + \eta d_r) - f(x_r) \leq c\eta \langle \nabla f(x_r), d_r \rangle$  for  $c \in (0, 1)$ , and then updates the iterate to  $x_r + \eta d_r$ . Our proposed conditions (14)–(15) have a similar form but are fundamentally different by replacing  $c\eta$  with  $C_{\text{ls}} n \eta^2$ . This distinction is a critical innovation to accommodate the high-dimensional network model, where the number of latent vectors grows with  $n$ . Accordingly, unlike  $c \in (0, 1)$  required in the Armijo rule, the constant  $C_{\text{ls}}$  can be chosen more flexibly and can be equal to or even greater than 1.

**5.2. Convergence Theory for Projected Gradient Descent.** This subsection presents the convergence theory for Algorithm 1. Because latent vectors are identifiable only up to orthogonal transformation  $\mathcal{O}(k)$ , we measure the distance between two matrices of latent vectors  $\hat{Z}$  and  $Z \in \mathbb{R}^{n \times k}$  by

$$\text{dist}(\hat{Z}, Z) := \min_{Q \in \mathcal{O}(k)} \|\hat{Z} - ZQ\|_{\text{F}}.$$

This is similarly considered in other studies [14, 22, 40], and it can be typically shown to be of the same order as  $\|\hat{Z}\hat{Z}^\top - ZZ^\top\|_{\text{F}}/\sqrt{n}$  [41]. Then for  $\hat{Y} = [\hat{Z}, \hat{\alpha}]$  and  $Y = [Z, \alpha]$ , we define the squared overall error as  $\text{dist}^2(\hat{Y}, Y) := \text{dist}^2(\hat{Z}, Z) + \|\hat{\alpha} - \alpha\|_2^2$ , where the discrepancy between  $\hat{\alpha}$  and  $\alpha$  is directly measured by the vector  $\ell_2$  norm.

To establish the convergence, we impose a regularity condition on the inputs of Algorithm 1 and discuss its implications afterwards.

CONDITION 3 (Inputs of Algorithm 1). Assume:

- (i) The initial estimate  $Y^0 = [Z^0, \alpha^0]$  satisfies (a)  $1_n^\top Z^0 = 0$ , (b)  $\text{dist}^2(Y^0, Y^*) \lesssim n^{1-\varsigma_0}$  for a constant  $\varsigma_0 \in (0, 1/2)$ , and (c)  $\|Y^0\|_{2 \rightarrow \infty} \leq b_0$  for a constant  $b_0 > 0$ .
- (ii) The initial step size  $\eta_{\text{init}}$  satisfies  $1/C_{\text{init}} \leq n\eta_{\text{init}} \leq C_{\text{init}}$  for a constant  $C_{\text{init}} > 1$ .
- (iii) The backtracking iteration limit  $R'$  satisfies  $R' \rightarrow \infty$  as  $n \rightarrow \infty$ .

To keep the convergence theory broadly applicable, Condition 3 (i) gives an abstract initialization condition on  $Y^0$ . In Section 5.4, we will provide a concrete example based on the singular value thresholding and verify Condition 3 (i) holds with high probability. We next explain the implications of the three requirements (a)–(c) in Condition 3 (i). First, the constraint  $1_n^\top Z^0 = 0$  ensures that the columns of  $Z^0$  are centered. This requirement is mild since any estimate can be centered without changing the induced likelihood value as discussed after Condition 1. Moreover, with this initialization, the next iterate also satisfies the centering constraint as  $1_n^\top Z^1 = 1_n^\top Z^0 - \eta_0 1_n^\top J_n \nabla_Z L(Y^0) = 0$  by  $1_n^\top J_n = 0$ . Therefore, throughout all the iterations in Algorithm 1, latent vectors remain centered, and the translational non-identifiability is avoided. Second, part (b) imposes an overall error bound on  $Y^0$ . It is similar to Assumption 8 on the overall error of initialization in [22]. In our problem setting, the required rate in [22] is slightly weaker as it reduces to  $\text{dist}^2(Y^0, Y^*) \leq cn$  for a sufficiently small  $c$ . Nevertheless, the sharper rate in Condition 3 (i) does not lead to a significant difference and can be shown to be satisfied by the initial estimator presented in Section 5.4. Third, part (c) implies that row-wise  $\ell_2$  norms of  $Y^0$  are uniformly bounded. Notably,  $b_0$  only needs to be a universal constant and does not rely on any unknown true model parameters. This differs from [22] that enforces boundedness by explicitly projecting each iterate onto a bounded set relying on the unknown truth.

Condition 3 (ii) implies that the initial learning rate should be of the order of  $1/n$ . It is a weak requirement because no precise constant needs to be specified, thanks to the adaptive search rules (14)–(15). This overcomes the implicit dependence on the unknown ground truth of step sizes in previous analysis; more technical details are discussed in Remark 8.

In Condition 3 (iii),  $R'$  represents the budget on the number of backtracking steps and is required only to diverge with  $n$ . This is simply to rule out pathological scenarios where the backtracking procedure would continue indefinitely. Setting a slow rate, such as  $R' \asymp \log n$ , would be practically innocuous. Actually, Section 5.3 will show that the backtracking can end in finite steps with high probability.

We are now ready to present the convergence guarantee for the output of Algorithm 1.

**THEOREM 2.** *Assume Conditions 1–3. For any constant  $\varepsilon > 0$ , there exist constants  $C > 0$ ,  $c_0 \in (0, 1)$ , and  $N_\varepsilon \in \mathbb{N}$  such that when  $n \geq N_\varepsilon$ ,*

$$\text{dist}^2(Y^r, \hat{Y}) \leq C(1 - c_0)^r \text{dist}^2(Y^0, \hat{Y})$$

*holds for any  $0 \leq r \leq R$  with probability  $1 - O(n^{-\varepsilon})$ , where  $\hat{Y} = [\hat{Z}, \hat{\alpha}]$  denotes any representative element in the equivalence class of the constrained maximum likelihood estimator defined in (5).*

Theorem 2 establishes an R-linear convergence guarantee for Algorithm 1. It implies that the distance between  $Y^r$  and  $\hat{Y}$  is bounded by  $(1 - c_0)^r$  which converges to 0 as  $r \rightarrow \infty$ . Therefore, as the number of iterations  $R$  increases, the output of Algorithm 1 converges to the constrained maximum likelihood estimator  $\hat{Y}$ , up to the equivalence class induced by  $\mathcal{O}(k)$ . Specifically, when  $R \gg \log n$ , the algorithmic error is negligible compared to the statistical error in Theorem 1. This suggests that the asymptotic distribution in Theorem 1 can

also hold for the algorithm output  $Y^R$  approximately, thereby justifying applying inferential procedures to  $Y^R$  in practice. This conclusion is substantially different from the convergence guarantee (Theorem 9) in [22] which essentially controls the distance between algorithm output  $Y^R$  and true model parameters  $Y^*$ . Because their target is different, the corresponding error bound in [22] mixes the statistical error with the algorithmic convergence error, and therefore does not directly justify the use of the inferential results in Theorem 1.

Interestingly, Theorem 2 does not explicitly depend on the constrained constant  $M$  in (5). This is non-trivial because Theorem 1 requires  $M$  to be sufficiently large to study  $\hat{Y}$ , and we remove the explicit projection onto an unknown bounded set compared to Algorithm 1 in [22]. This is made possible by two key theoretical results. First, as discussed in Remark 5, we show the definition of  $\hat{Y}$  is not sensitive to a particular choice of  $M$ , provided  $M$  is large enough. Second, we develop new theoretical techniques showing that  $\|Y^r\|_{2 \rightarrow \infty}$  remains in a uniformly bounded region throughout the iterations with high probability.

The boundedness phenomenon is related to the implicit regularization noted by [23] under different models, but the analysis here is fundamentally different. Specifically, our framework must tackle the intrinsic non-linearity with respect to  $Y$ , e.g., the link function in (11) is non-linear. Also, it needs to accommodate our fully data-adaptive scheme that does not depend on unknown true parameters. These challenges cannot be directly handled by existing techniques. As a by-product, our analysis bypasses the construction of the leave-one-out sequences in [23], which could be of independent theoretical interest. These efforts not only make technical contributions but also further support the practical relevance of Algorithm 1 under more flexible settings.

The constant  $c_0 \in (0, 1)$  in Theorem 2 quantifies the contraction rate of the error upper bound. Its explicit expression is technically involved, as it reflects the adaptiveness of our algorithm and generality of our distributional framework, so we defer it to the Supplementary Material; see Remark F.3. Nevertheless, we mention that the derived formula shows that the convergence rate depends on the same key model characteristics as in [22]. In particular,  $c_0$  decreases as the condition number of  $Z^{*\top}Z^*/n$  or  $M_1$  in Condition 1 increases. Thus, the obtained convergence rate is consistent with that in [22] even under the more adaptive and general scenarios considered in this paper.

REMARK 7. Although the algorithmic structure of Algorithm 1 is similar to that in [22], we emphasize the underlying proofs of Theorem 2 follow substantially different arguments. First, we directly deal with the non-convex loss over  $Y = [Z, \alpha]$  and explicitly disentangle the statistical and algorithmic errors. Second, our proof of Theorem 2 not only establishes the F-norm convergence but also shows uniform boundedness of  $y_i^r$  across all iterations. The latter cannot be shown by existing techniques. Third, all of our convergence conclusions are fully data-adaptive and do not require unknown information about true parameters. Fourth, to fulfill the requirements of the initialization, we develop new data-adaptive singular value thresholding estimator in Section 5.4 below. Taken together, these features show that our analysis is a genuinely different framework with both theoretical and practical advantages.

5.3. *Implementation Details of Projected Gradient Descent.* This subsection discusses several implementation details and variants of Algorithm 1. First, Corollary 2 will show that setting a backtracking budget  $R'$  would not impact reaching an acceptable step size with high probability.

COROLLARY 2. *The line search step in Algorithm 1 has the following guarantees:*

- (i) *Assume Conditions 1–3. For any  $\varepsilon > 0$ , there exists  $N_\varepsilon \in \mathbb{N}$ , such that when  $n \geq N_\varepsilon$ , the line search stage terminates within  $R'$  steps across all iterations in Algorithm 1, with probability  $1 - O(n^{-\varepsilon})$ .*

- (ii) Assume Conditions 1–2 and Condition 3 (i). Additionally, assume that the initial estimate  $Y^0 = [Z^0, \alpha^0]$  satisfies  $\|Z^0 - Z^* Q_z\|_{2 \rightarrow \infty} + \|\alpha^0 - \alpha^*\|_\infty \lesssim \zeta_{0,n}$  for some sequence  $\zeta_{0,n} \ll 1$  and some  $Q_z \in \mathcal{O}(k)$ . Choose the initial step size as

$$(16) \quad \eta_{\text{init}} = \frac{1}{6 \max_{1 \leq i < j \leq n} \{1 - \ell''(\Theta_{ij}^0)\}} \cdot \min \left\{ \frac{1}{\|Z^0\|_{\text{op}}^2}, \frac{1}{n} \right\},$$

where  $\Theta_{ij}^0 = \alpha_i^0 + \alpha_j^0 + \langle z_i^0, z_j^0 \rangle$ . Then  $\eta_{\text{init}}$  satisfies Condition 3 (ii), and for any  $\varepsilon > 0$ , there exists  $N_\varepsilon \in \mathbb{N}$ , such that when  $n \geq N_\varepsilon$ , the line search conditions (14)–(15) are satisfied at  $\eta = \eta_{\text{init}}$  for all iterations with probability  $1 - O(n^{-\varepsilon})$ .

Case (i) in Corollary 2 indicates that when the backtracking budget  $R'$  diverges with  $n$ , the imposed cap would not interfere with reaching a desired step size with high probability. Case (ii) considers a scenario with a stronger initialization. Specifically, if a sharper two-to-infinity error bound for  $Y^0$  is available, we can construct a closed-form choice of  $\eta_{\text{init}}$  in (16) such that the line search conditions (14)–(15) hold with high probability. Thus,  $\eta_r = \eta_{\text{init}}$  throughout, and the backtracking loop needs not to be triggered. This two-to-infinity-error assumption is much stronger than the row-wise boundedness in Condition 3. It could hold under a stronger structural assumption on  $\mathbb{E}(A)$ , such as low rank [7]. Notably,  $\eta_{\text{init}}$  in (16) takes a form similar to the choice in [22]; see Remark 8 for more discussions. This helps explain why step sizes of a similar form have worked well in prior studies [14, 22].

REMARK 8 (Comparison with step sizes in [22]). Ma, Ma and Yuan [22] set step sizes for  $Z$  and  $\alpha$  as  $\eta_Z = \eta / \|Z^0\|_{\text{op}}^2$  and  $\eta_\alpha = \eta / (2n)$ , respectively, where  $\eta$  is a hyperparameter. To establish theoretical guarantees,  $\eta$  is required to satisfy inequalities that involve unknown model parameters; see, e.g., the last three inequalities in their proof of Lemma 25. In contrast, our proposed line search rules (14) and (15) determine the step size adaptively from the data and avoid the need to specify such unknown constants. Moreover, for the choice in (16), we have  $\eta_{\text{init}} \asymp \min\{1/\|Z^0\|_{\text{op}}^2, 1/n\}$ , matching the choices in [22] up to a multiplicative constant.

For clarity of exposition, we present the projected gradient descent Algorithm 1 in a streamlined form above. We emphasize that our analytical framework readily accommodates different variations in practice and next discuss several examples below.

REMARK 9 (Component-wise step sizes). The above discussions consider a common step size for updating both  $Z$  and  $\alpha$  in each iteration. But our results can be straightforwardly generalized when considering component-wise step sizes. In particular, we can replace  $Y + \eta d(Y)$  and  $Y + \eta d_i(Y)$  in (14)–(15) with  $Y + d(Y)\eta_D$  and  $Y + d_i(Y)\eta_D$ , respectively, where  $\eta_D = \text{blkdiag}(\eta_Z, \dots, \eta_Z, \eta_\alpha) \in \mathbb{R}^{(k+1) \times (k+1)}$ . Then we can conduct the line search with  $\eta_Z = \beta \eta_Z$  and  $\eta_\alpha = \beta \eta_\alpha$  similarly. All of our developments and conclusions extend with only routine notational modifications.

REMARK 10 (Iteration-varying initial step sizes). The above discussions use a common initial step size  $\eta_{\text{init}}$  across all iterations  $1 \leq r \leq R$ . More generally, our framework also allows  $\eta_{\text{init}}$  to vary with  $r$ , which remains theoretically valid and may provide additional adaptiveness. For example, Case (ii) in Corollary 2 motivates constructing  $\eta_{\text{init},r}$  in the same form as (16), but with  $Y^0 = [Z^0, \alpha^0]$  replaced by  $Y^r = [Z^r, \alpha^r]$  at the  $r$ -th iteration. The same argument then shows that  $\eta_{\text{init},r}$  satisfies Condition 3 (i) with high probability, and the convergence guarantee continues to hold, that is,  $Y^r$  approaches  $Y^*$  up to the identifiability constraint as  $r$  increases. As a result, we expect  $\eta_r = \eta_{\text{init},r}$  when  $r$  is large, thereby reducing the computational cost from triggering the backtracking loop.

REMARK 11 (Stopping criteria). Besides using a targeted  $R$  for termination, another common practice in gradient-descent-based algorithms is to set stopping criteria. Our theoretical analysis is flexible and can be extended to justify that scenario too. As an example, one widely used criterion is to stop at the  $r$ -th iteration if  $\|\nabla_Y L(Y^r)\|_F \leq \epsilon$  for a prespecified  $\epsilon$ . Our proof of Theorem 2 shows that with high probability, the iterates  $Y^r$  in Algorithm 1 satisfy  $\text{dist}(Y^r, \hat{Y}) \asymp n^{-1} \|\nabla_Y L(Y^r)\|_F$ , so  $\|\nabla_Y L(Y^r)\|_F \leq \epsilon$  guarantees  $\text{dist}(Y^r, \hat{Y}) = O_p(\epsilon/n)$ . Hence when  $\epsilon$  is chosen sufficiently small, we expect the difference between  $Y^r$  and  $\hat{Y}$  to be ignorable for practical use. This provides theoretical justification for using the gradient norm as a practical stopping criterion.

5.4. *Initialization: Range-Adaptive Singular Value Thresholding*. As mentioned in Section 3.2, the spectral-based universal singular value thresholding [8] is one of the most widely used approaches for initializing the projected gradient descent under latent space models [14, 19, 49]. A representative example is the initialization method (Algorithm 3) in [22], which builds on the USVT under the logic transform. However, similarly to the challenges in the projected gradient descent procedure, this approach requires an explicit projection step relying on unknown model parameters to obtain the theoretical guarantee.

To obtain an initial estimator that is practically applicable while still retaining the theoretical guarantee, we propose a Range-Adaptive Singular Value Thresholding (RA-SVT) method, with a pseudo-code summary in Algorithm 2. Specifically, after applying the singular value thresholding to the observed matrix  $A$  and obtaining  $\tilde{E}$ , we construct the adaptive interval

$$(17) \quad [\tilde{E}_{(\gamma_n)}, \tilde{E}_{(n^2-\gamma_n)}] \cap [\tilde{E}_{(l_1)}, \tilde{E}_{(l_2)}],$$

where  $\tilde{E}_{(1)} \leq \dots \leq \tilde{E}_{(n^2)}$  denote the ordered statistics of all elements in  $\{\tilde{E}_{ij} : 1 \leq i, j \leq n\}$ ,  $\gamma_n$  is a hyperparameter to trim extreme values, and  $1 \leq l_1 < l_2 \leq n^2$  denote the smallest and largest indices such that  $\mu^{-1}(e)$  is well-defined for  $e \in [\tilde{E}_{(l_1)}, \tilde{E}_{(l_2)}]$  and the link function  $\mu(\cdot)$  in (11).

The two intervals in (17) serve two different purposes. The first one  $[\tilde{E}_{(\gamma_n)}, \tilde{E}_{(n^2-\gamma_n)}]$  trims extreme values in a data-adaptive way, while the second interval  $[\tilde{E}_{(l_1)}, \tilde{E}_{(l_2)}]$  constrains (17) to stay inside the image of  $\mu$ , so that  $\mu^{-1}(\cdot)$  can be applied to any projected value. Further discussions are given after Condition 4 below. Our proposed Algorithm 2 is connected to the initialization method in [22] when the adaptive interval (17) is replaced by the fixed interval  $[e^{-M_1}/2, 1/2]$  and  $\mu(x) = e^x/(1+e^x)$ . The advantage of our construction is that the adaptive interval  $[\tilde{E}_{(\gamma_n)}, \tilde{E}_{(n^2-\gamma_n)}]$  produces a suitably bounded interval without relying on unknown model parameters.

5.5. *Asymptotic Theory for Range-Adaptive Singular Value Thresholding*. We next establish the asymptotic guarantee for the proposed RA-SVT estimator  $\hat{Y} = [\hat{Z}, \hat{\alpha}]$  from Algorithm 2. The goal is to show that  $\hat{Y}$  satisfies the initialization requirement in Condition 3 under suitable conditions and tuning parameters. To this end, we impose regularity conditions on the link function in (11) and the hyperparameters in Conditions 4 and 5 below.

CONDITION 4 (Link function). Assume  $\mu(\theta)$  in (11) satisfies the following conditions.

- (i) The function  $\mu(\theta)$  is continuously differentiable with its derivative denoted by  $\mu'(\theta)$ . Moreover, for any constant  $b > 0$ , there exist constants  $\kappa_4(b), \kappa_5(b) > 0$  such that

$$\kappa_4(b) \leq \mu'(\theta) \leq \kappa_5(b) \quad \text{for all } \theta \in [-b, b].$$

- (ii) For any  $t \geq 0$ ,  $\Pr(|A_{ij} - \mu(\Theta_{ij}^*)| > t) \leq 2 \exp(-(t/K)^s)$  for fixed constants  $K, s > 0$ , which, without loss of generality, can be assumed to be same as those in Condition 2 (ii).

---

**Algorithm 2:** Range-Adaptive Singular Value Thresholding
 

---

**Input:** Data:  $A \in \mathbb{R}^{n \times n}$ . Hyperparameters:  $\tau_n, \gamma_n$ .

- 1 Let  $\sum_{i=1}^n \sigma_i u_i v_i^\top$  denote the singular value decomposition of  $A$ .
- 2 Let  $\tilde{E} = \sum_{\{i: \sigma_i > \tau_n\}} \sigma_i u_i v_i^\top$ . Elementwisely project  $\tilde{E}$  onto (17) to obtain  $\hat{E}$ .
- 3 Let  $\hat{\Theta} \in \mathbb{R}^{n \times n}$  with entries  $\hat{\Theta}_{ij} = \mu^{-1}(\hat{E}_{ij})$  across  $1 \leq i, j \leq n$ .
- 4 Let  $\hat{\alpha} = (nI_n + 1_n 1_n^\top)^{-1} \hat{\Theta} 1_n$ .
- 5 Let  $\hat{Z} = \mathcal{S}_k(\hat{\Theta} - \hat{\alpha} 1_n^\top - 1_n \hat{\alpha}^\top)$ , where  $\mathcal{S}_k(\cdot)$  denotes the operator that takes the top- $k$  positively truncated square root of the input matrix, formally defined in (H.1) in the Supplementary Material.

**Output:**  $\hat{Y} = [\hat{Z}, \hat{\alpha}]$ .

---

Under the natural exponential family distributions with canonical link functions, Condition 4 follows directly from Condition 2. Specifically, in that setting,  $\mu'(\theta) = -\ell''(\theta; x)$  and  $A_{ij} - \mu(\Theta_{ij}^*) = \ell'(\Theta_{ij}^*; A_{ij})$ . Thus, Condition 4 is equivalent to Condition 2 with  $\kappa_4(b) = \kappa_1(b)$  and  $\kappa_5(b) = \kappa_2(b)$ , suggesting no extra restrictions in the canonical setting. Moreover, Condition 4 (i) guarantees the invertibility of  $\mu(\cdot)$  and existence of indexes  $l_1$  and  $l_2$  in (17). In particular, it implies that  $\mu(\cdot)$  is continuous and strictly increasing over any closed interval on  $\mathbb{R}$ . Hence  $\mu(\mathbb{R})$ , the image of  $\mu(\cdot)$  over  $\mathbb{R}$ , is an interval, and its inverse function  $\mu^{-1}(x)$  is well-defined for all  $x \in \mu(\mathbb{R})$ . Therefore,  $l_1$  and  $l_2$  in (17) exist and are easy to identify. For example, if  $\mu(\mathbb{R}) = (a, b)$ ,  $l_1$  and  $l_2$  are simply the smallest and largest indices such that  $\tilde{E}_{(l_1)} > a$  and  $\tilde{E}_{(l_2)} < b$ . This guarantees that applying  $\mu^{-1}(\cdot)$  after the projection onto the adaptive interval (17) is valid. Canonical link functions, such as  $\mu(x) = e^x / (1 + e^x)$  for Bernoulli distribution and  $\mu(x) = e^x$  for Poisson distribution, indeed satisfy Condition 4 (i).

CONDITION 5 (Tuning parameters). The tuning parameters of Algorithm 2 satisfy:

- (i) Threshold:  $n^{\frac{1}{2}} \ll \tau_n \ll n^{\frac{1}{2} + \frac{1}{k+3}}$ ;
- (ii) Trimming quantile:  $\tau_n n^{\frac{3}{2} - \frac{1}{k+3}} \ll \gamma_n \ll n^2$ .

The threshold  $\tau_n$  controls how much truncation is applied to  $A$ . Original USVT [8] recommends a threshold of order  $n^{1/2}$ , which is slightly smaller than our lower bound  $\tau_n \gg n^{1/2}$  in Condition 5. This difference arises because [8] assumes that entries of the observed data matrix are bounded with probability one, whereas our framework also accommodates unbounded data with a unified analysis. In practice, however, the gap is insignificant. For example, we can choose  $\tau_n = n^{1/2} \log n$ , which differs from  $n^{1/2}$  only by a slow  $\log n$  rate and already satisfies Condition 5 (i). Condition 5 (i) is stated as a range instead of a fixed choice for flexibility and generalizability. Intuitively,  $\tau_n$  should be sufficiently small to preserve useful signals in  $\mathbb{E}(A)$ , but within a suitable range, a slightly larger  $\tau_n$  may help remove more noises. The optimal choice of  $\tau_n$  could be an interesting question. But this is not pursued in this paper as Algorithm 2 is only used as an initialization for Algorithm 1.

The trimming quantile  $\gamma_n$  controls the length of the adaptive projection interval (17). For a fixed  $\tilde{E}$ , increasing  $\gamma_n$  shortens  $[\tilde{E}_{(\gamma_n)}, \tilde{E}_{(n^2 - \gamma_n)}]$ , and then typically shortens (17) too. The admissible range of  $\gamma_n$  in Condition 5 (ii) reflects a tradeoff. On the one hand,  $\gamma_n$  needs to be sufficiently large to screen out extreme entries in  $\tilde{E}$  and produce a bounded interval, which is essential for effective regularization. Technically, the lower bound in Condition 5 arises from our derived error rate  $\|\tilde{E} - \mu(\Theta^*)\|_{\mathbb{F}}^2 = O_p(\tau_n n^{\frac{3}{2} - \frac{1}{k+3}})$ . Our intuition of setting  $\tau_n n^{\frac{3}{2} - \frac{1}{k+3}}$

as the lower bound is that it delineates the order of the overall estimation error in  $\tilde{E}$ , and thus serves as a useful benchmark for the minimum trimming level. On the other hand, if  $\gamma_n$  is too large, the entries in  $\mu(\Theta^*)$  are increasingly likely to fall outside the interval in (17), and the induced bound of  $\text{dist}^2(\mathring{Y}, Y^*)$  in (18) below will deteriorate. A suitably large  $\gamma_n$  allows (17) to cover the entries in  $\mu(\Theta^*)$  asymptotically without knowing  $\Theta^*$  (or  $M_1$  in Condition 1). The upper bound  $\gamma_n \ll n^2$  is natural, because the induced error bound in (18) is consistent with existing results; see more discussions below.

**THEOREM 3.** *Assume Conditions 1, 2, 4, and 5. For any constant  $\varepsilon > 0$ , there exist constants  $C > 0$  and  $N_\varepsilon \in \mathbb{N}$  such that when  $n \geq N_\varepsilon$ ,*

$$(18) \quad \text{dist}^2(\mathring{Y}, Y^*) \leq \frac{C\gamma_n}{n} \quad \text{and} \quad \|\mathring{Y}\|_{2 \rightarrow \infty} \leq C$$

with probability  $1 - O(n^{-\varepsilon})$ .

Theorem 3 establishes two key bounds for  $\mathring{Y} = [\mathring{Z}, \mathring{\alpha}]$ . The first bound implies that the squared Frobenius norm error for estimating  $Y^*$  is  $o(n)$ , as  $\gamma_n = o(n^2)$  by Condition 5. This is consistent with conclusions in [8] and [22]. The second bound shows that  $\|\mathring{Y}\|_{2 \rightarrow \infty}$  remains bounded. Such a result is essential for fulfilling the requirement in Condition 3 but has not been established in [8] or [22]. In summary, Theorem 3 suggests that there exist choices of  $\gamma_n$  and  $\tau_n$  such that the resulting estimator  $\mathring{Y}$  satisfies the requirements of initial estimates in Condition 3. For example, we can set

$$(19) \quad \gamma_n \asymp n^{2-\varsigma_0} \text{ for any } \varsigma_0 \in (0, 1/(k+3)), \text{ and any } n^{\frac{1}{2}} \ll \tau_n \ll n^{\frac{1}{2} + \frac{1}{k+3} - \varsigma_0}.$$

As discussed after Corollary 2, stronger conclusions, such as consistent two-to-infinity error control, may be available under additional structural assumptions on the expected adjacency matrix  $\mathbb{E}(A)$ . However, such assumptions are generally unavailable or hard to justify given a nonlinear link in (11). Instead, Theorem 3 is tailored to the error control actually needed for the initialization under relatively weak structural assumptions.

**6. Simulations.** This section provides simulation studies to assess both the algorithmic performance and asymptotic theory developed in this paper. We begin with describing the simulation setup used throughout the section. Section 6.1 studies the convergence behavior, and Section 6.2 examines the distribution of the obtained estimator.

*Simulation setup.* Following [22], we generate  $\alpha^*$  by first sampling  $\tilde{\alpha} \in \mathbb{R}^n$  with independent entries from the uniform distribution on  $[1, 3]$  and then normalizing it to  $\alpha^* = \tilde{\alpha}/(1_n^\top \tilde{\alpha})$ . In addition, we let  $k = 2$  and generate random  $\tilde{Z} \in \mathbb{R}^{n \times k}$  with independent entries following the standard normal truncated to the interval  $[-2, 2]$ . Then we construct  $Z^* = 0.5\sqrt{n}\tilde{U}$ , where  $\tilde{U}$  denotes the left singular vectors of the centered matrix  $J_n \tilde{Z}$  with  $J_n$  defined as in (13). This construction yields two equal nonzero eigenvalues of  $Z^{*\top} Z^*$ , thereby placing the simulations in the challenging repeated-eigenvalue regime studied in this paper.

Given  $(Z^*, \alpha^*)$ , we generate network data  $A$  from the model (1) under three common distributions, Poisson, Bernoulli, and Gaussian with their respective canonical links. Under each distribution, we take  $n \in \{500, 1000, 2000, 4000\}$ . The main text presents results under the Poisson distribution, while the results under the Bernoulli and Gaussian distributions are similar and are deferred to Section J of the Supplementary Material.

The proposed projected gradient descent (Algorithm 1) is implemented with  $C_{1s} = 1, \beta = 0.5, R = 2000$ , and  $R'$  equal to the ceiling of  $\log n$ . The initial estimator  $Y^0$  is constructed by Algorithm 2. Following (19), we choose  $\gamma_n = 0.1 n^{2-\varsigma_0}$  with  $\varsigma_0 = 1/(k+4)$  and  $\tau_n = (v_n n \log n)^{1/2}$  with  $v_n = \sum_{1 \leq i, j \leq n} A_{ij}/n^2$ . Here  $\tau_n$  satisfies (19) with high probability, as

$v_n$  concentrates around a constant. Following Remark 11, we adopt an early stopping criterion that  $S_{\max}^r := \max_{1 \leq i \leq n, 1 \leq j \leq k+1} |\nabla_{y_{ij}} L(Y^r)| \leq 0.01$ , where  $\nabla_{y_{ij}} L(Y)$  denotes the partial derivative of  $L(Y)$  with respect to  $y_{ij}$ , i.e., the  $(i, j)$ -th entry of  $\nabla_Y L(Y) \in \mathbb{R}^{n \times (k+1)}$ .

**6.1. Algorithmic Performance of the Projected Gradient Descent.** We examine the adaptivity and computational trade-off of the proposed algorithm. To this end, we vary the initial step size and compare the adaptive procedure with a fixed-step counterpart. Specifically, we take  $\eta_0$  to be six times (16), which serves as a baseline step size determined by the initial estimator, and consider four scales  $\eta_{\text{init}}/\eta_0 \in \{10, 5, 1, 1/5\}$ . The fixed-step counterpart of Algorithm 1 sets  $\eta_r = \eta_{\text{init}}$  throughout the iterations, equivalent to skipping lines 5–9 in Algorithm 1. Each configuration is evaluated over 100 Monte Carlo replications. To measure convergence, we use  $S_{\max}^r$  as a quantitative measure, because by Remark 11,  $S_{\max}^r$  converges to 0 if and only if  $Y^r$  approximates the maximum likelihood estimator  $\hat{Y}$  up to the identifiability constraints. Accordingly, we let  $R_{\text{conv}}$  denote the smallest iteration  $r$  such that  $S_{\max}^r \leq 0.01$ , and declare convergence if  $R_{\text{conv}} \leq R = 2000$ .

Table 1 presents the empirical convergence proportions under both adaptive and fixed step sizes. Using the adaptive step size, the projected gradient descent algorithm converges reliably under all values of  $\eta_{\text{init}}$ . In contrast, the fixed-step method fails to converge when  $\eta_{\text{init}} \in \{10, 5\}$ , indicating high sensitivity to the initial step size.

TABLE 1  
Empirical convergence proportions over 100 Monte Carlo replications under the Poisson model.

| $n$  | Adaptive step size          |      |      |      | Fixed step size             |      |      |      |
|------|-----------------------------|------|------|------|-----------------------------|------|------|------|
|      | $\eta_{\text{init}}/\eta_0$ |      |      |      | $\eta_{\text{init}}/\eta_0$ |      |      |      |
|      | 10                          | 5    | 1    | 1/5  | 10                          | 5    | 1    | 1/5  |
| 500  | 1.00                        | 1.00 | 1.00 | 1.00 | 0.00                        | 0.00 | 1.00 | 1.00 |
| 1000 | 1.00                        | 1.00 | 1.00 | 1.00 | 0.00                        | 0.00 | 1.00 | 1.00 |
| 2000 | 1.00                        | 1.00 | 1.00 | 1.00 | 0.00                        | 0.00 | 1.00 | 1.00 |
| 4000 | 1.00                        | 1.00 | 1.00 | 1.00 | 0.00                        | 0.00 | 1.00 | 1.00 |

To explain the patterns in Table 1, Figure 1 presents  $S_{\max}^r$  against the iteration index  $r$  for a randomly chosen replication with  $n = 1000$  and  $\eta_{\text{init}}/\eta_0 \in \{10, 5\}$ . Figure 1(a) shows that the maximum absolute score steadily decreases to 0 when using the adaptive step size. By contrast, Figure 1(b) shows that for the fixed-step method,  $S_{\max}^r$  stagnates at a non-zero level when  $\eta_{\text{init}} = 5\eta_0$ , and even diverges when  $\eta_{\text{init}} = 10\eta_0$ . This suggests that the produced estimator can be far from  $\hat{Y}$ . These different trajectories demonstrate the effectiveness and adaptivity of the proposed line search method.

Although the adaptive method converges across different  $\eta_{\text{init}}$ , the choice still affects computational efficiency. Figure 2(a) shows the distribution of the number of gradient descent iterations to convergence, i.e.,  $R_{\text{conv}}$ , versus different  $\eta_{\text{init}}/\eta_0$ . When  $\eta_{\text{init}}$  is small, the updates are more conservative, and  $R_{\text{conv}}$  is correspondingly larger. As  $\eta_{\text{init}}$  increases,  $R_{\text{conv}}$  decreases significantly. Moreover, Figure 2(b) presents the empirical distribution of the backtracking steps per iteration. For each  $\eta_{\text{init}}/\eta_0$ , the corresponding boxplot collapses to a line segment, because the backtracking steps remain identical across all gradient descent iterations and Monte Carlo replications. The results suggest that more backtracking steps are consistently needed when  $\eta_{\text{init}}/\eta_0$  is large. In summary, Figure 2 reveals the computational trade-off that larger initial step sizes reduce the number of iterations to convergence but could incur more backtracking steps. A moderately large initial step size offers a favorable balance between rapid descent and limited backtracking.

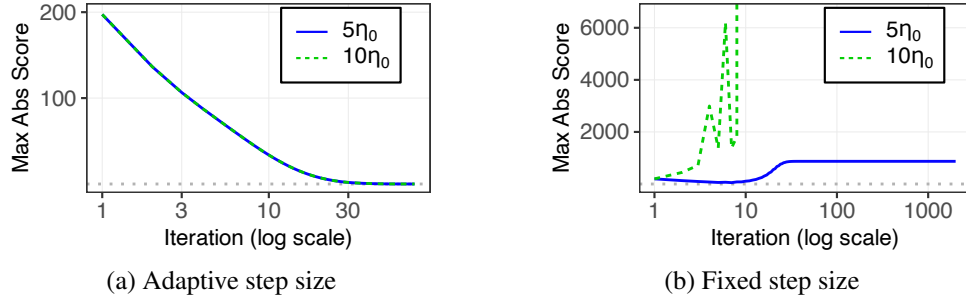


Fig 1: Maximum absolute score  $S_{\max}^r$  versus iteration  $r$  under the Poisson model with  $n = 1000$  in one Monte Carlo replication. Panels (a) and (b) correspond to the adaptive and fixed step sizes, respectively. The gray dotted line marks the stopping threshold 0.01.

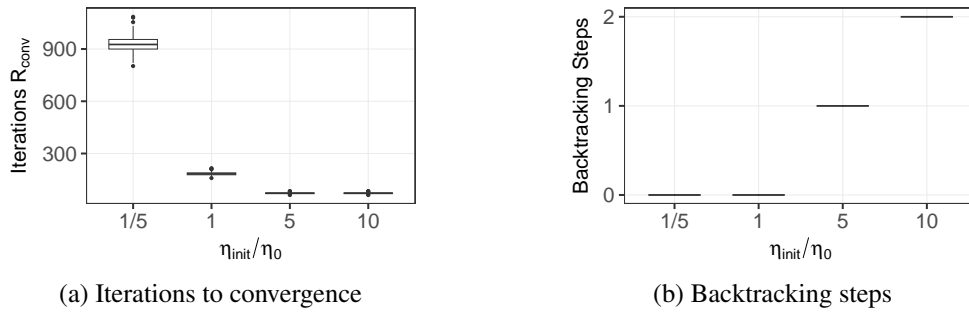


Fig 2: Computational trade-off under the adaptive step size for the Poisson model with  $n = 1000$  over 100 Monte Carlo replications. Panel (a) shows the boxplot of  $R_{\text{conv}}$  versus  $\eta_{\text{init}}/\eta_0$ . Panel (b) shows the boxplot of the backtracking steps per iteration versus  $\eta_{\text{init}}/\eta_0$ .

**6.2. Asymptotic Distribution.** We next present the empirical distribution of the obtained estimator and examine whether it aligns with the asymptotic theory in Theorem 1. To this end, it suffices to consider the adaptive step size with  $\eta_{\text{init}} = \eta_0$  since the convergence behavior is stable as shown in Section 6.1. Throughout this subsection, each setting is evaluated over 200 Monte Carlo replications.

We consider two representative estimands. The first is an entrywise latent-vector parameter. Specifically, consider  $z_{11}^*$ , the first coordinate of the node 1 latent vector. This corresponds to taking  $g(y_1) = \langle e_1^{(k+1)}, y_1 \rangle$  in Corollary 1, where  $e_1^{(k+1)} \in \mathbb{R}^{k+1}$  is the standard basis vector for the first coordinate in the  $(k+1)$ -dimensional space. It follows that the standardized statistic  $t(\hat{z}_{q,11}) := (\hat{z}_{q,11} - z_{11}^*)/\widehat{\text{se}}(\hat{z}_{q,11}) \xrightarrow{d} \mathcal{N}(0, 1)$  with  $\widehat{\text{se}}(\hat{z}_{q,11}) := \{e_1^{(k+1)\top} \Sigma_1(\hat{Y}_q)^{-1} e_1^{(k+1)}\}^{1/2}$ . Second, we consider a nonlinear transformation corresponding to the edge mean  $\mu(\Theta_{12}^*)$ . By Corollary 1, we construct the standardized statistic  $t(\hat{\mu}_{12}) := \{\mu(\hat{\Theta}_{12}) - \mu(\Theta_{12}^*)\}/\widehat{\text{se}}(\hat{\mu}_{12})$ , where  $\hat{\mu}_{12} := \mu(\hat{\Theta}_{12})$  and  $\widehat{\text{se}}(\hat{\mu}_{12})$  is defined in (12).

Figure 3 displays the QQ plots of  $t(\hat{z}_{q,11})$  against the standard normal  $\mathcal{N}(0, 1)$ , and Figure 4 presents the corresponding QQ plots for  $t(\hat{\mu}_{12})$ . In both cases, the empirical distributions of the standardized statistics closely align with the standard normal distribution. This supports the normal approximations by our asymptotic theory. Notably, the results are obtained when  $Z^{*\top} Z^*$  has repeated eigenvalues, demonstrating that a distinct-eigenvalue assumption is not essential for the asymptotic distributions considered here.

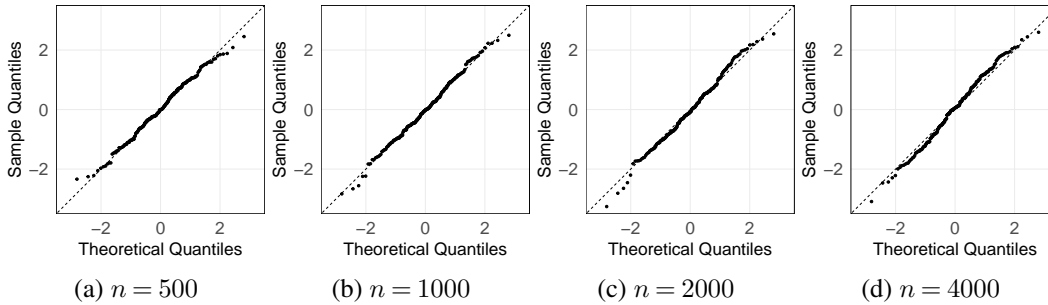


Fig 3: QQ plots of  $t(\hat{z}_{q,11})$  against  $\mathcal{N}(0, 1)$  under the Poisson model.

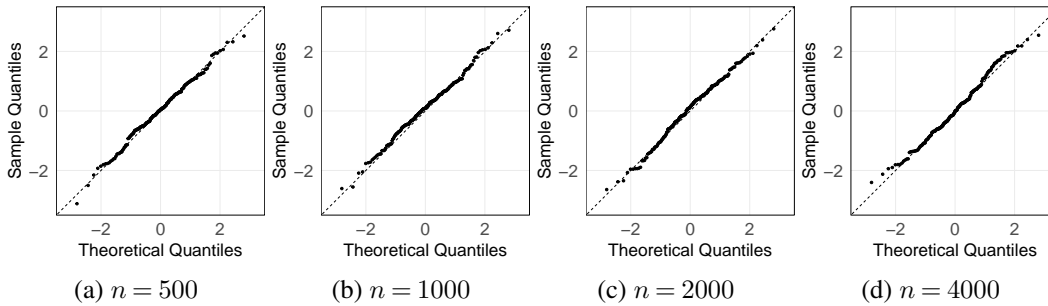


Fig 4: QQ plots of  $t(\hat{\mu}_{12})$  against  $\mathcal{N}(0, 1)$  under the Poisson model.

**7. Data Analysis.** To illustrate the proposed inference procedures, we analyze the New York Citi Bike dataset [9]. The raw data record rides between bike stations in New York City. Each ride contains two stations and a start time. We aim to compare the travel patterns during two commuting peak periods 8:00-9:00 and 18:00-19:00 on the weekday August 1st, 2019. We preprocess the data by keeping the rides that last between one minute and 3 hours and focusing on stations whose total degrees are at least one in both hours. The processed data contains 703 bike stations and 7,426 and 9,264 rides over the two peak hours, respectively.

For each hour, we construct a weighted network, where the network nodes represent stations, and the edge weight between two stations is the number of rides between them during that hour. We fit the proposed model separately to the two hourly networks using two-dimensional latent vectors under a Poisson model. This model choice is natural because the edge weights are count-valued. Figure 5 summarizes the estimation results.

Figure 5(a) visualizes the estimated latent positions for the morning network. It clearly shows three clusters that align well with the geographic borough structure of the stations. This alignment suggests that the fitted model captures meaningful and interpretable latent structure from the observed network. The evening network exhibits a similar pattern. Due to space limitation, the detailed results are deferred to the Supplementary Material, along with a reference map of true station locations for comparison.

Figures 5(b) and 5(c) present heatmaps of inner products between estimated latent vectors for the two networks. Specifically, the  $(i, j)$ -th entry of each heatmap corresponds to  $\langle \hat{z}_{1,i}, \hat{z}_{1,j} \rangle$  or  $\langle \hat{z}_{2,i}, \hat{z}_{2,j} \rangle$ , where  $\hat{z}_{1,i}$  and  $\hat{z}_{2,i}$  denote the estimated latent vectors for station  $i$  in the morning and evening networks, respectively. These inner products measure the latent affinity between stations after adjusting for node-specific baseline effects and are informative for understanding fundamental travel patterns. Both heatmaps reveal noticeable block structure that is consistent with the three-borough clustering pattern in Figure 5(a).

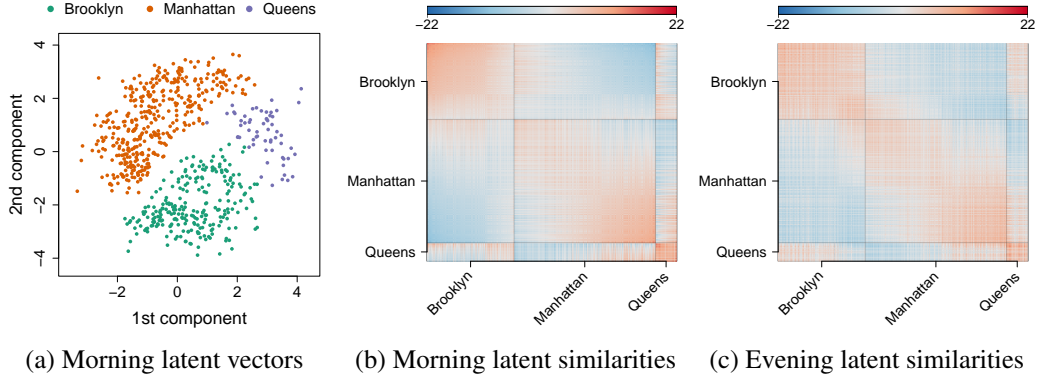


Fig 5: Estimation results. Panel (a) visualizes the estimated latent positions for the morning network. Each point is colored based on which borough the corresponding bike station is located. Panels (b) and (c) show two heatmaps over estimated latent similarity matrices, whose  $(i, j)$ -th entry is the inner product of the latent vectors for stations  $i$  and  $j$ .

In addition to estimating each network individually, comparing the morning and evening networks can further provide insights into how urban mobility patterns change across commuting periods. As a first step, we examine the raw difference between the two latent similarity matrices, presented as the heatmap in Figure 6(a). This raw difference matrix shows more pronounced patterns in the between-borough block compared to the single-network heatmaps in Figures 5. But the changes span across all station pairs, hindering clear interpretation.

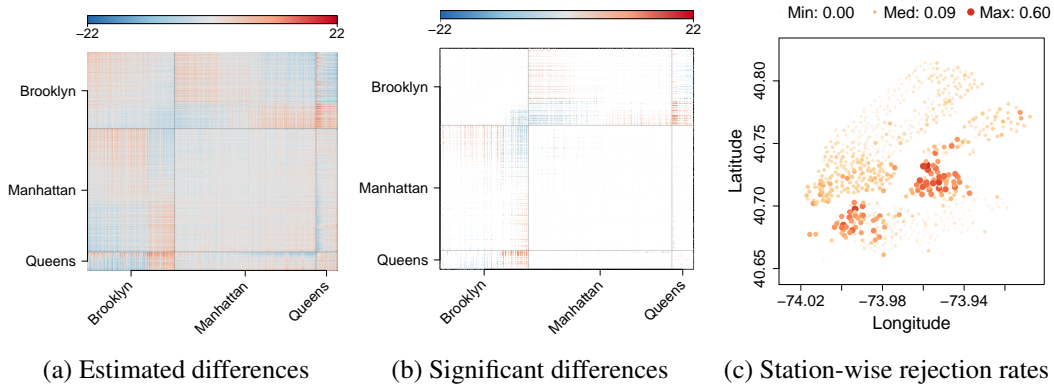


Fig 6: Two-sample comparison. Panel (a) displays the difference of the latent similarity matrices in the morning and evening hours. Panel (b) displays the same matrix after masking the entries that are insignificant after the Benjamini–Hochberg correction in white. Panel (c) shows the geographic locations of the stations, where the size and color of station  $i$  encode the proportion of the rejected two-sample tests involving station  $i$ .

To identify significant differences, we perform pairwise two-sample tests for differences in latent similarities between the two periods. Specifically, for each pair of stations  $(i, j)$ , we test whether  $\langle z_{1,i}, z_{1,j} \rangle$  and  $\langle z_{2,i}, z_{2,j} \rangle$  differ based on the estimator  $\langle \hat{z}_{1,i}, \hat{z}_{1,j} \rangle - \langle \hat{z}_{2,i}, \hat{z}_{2,j} \rangle$ . Each test is constructed from the asymptotic results in Theorem 1 and Corollary 1. Given the  $n(n-1)/2$  pairwise comparisons, we apply the Benjamini–Hochberg procedure at the level 0.05 to filter insignificant pairs.

Figure 6(b) displays the matrix of significant pairwise differences, with insignificant entries masked out by white color. In contrast to the raw difference heatmap, the statistically significant changes are concentrated primarily in off-diagonal blocks corresponding to between-borough station pairs. This observation indicates that morning–evening travel differences are driven more by inter-borough connectivity than by within-borough rides.

Figure 6(c) provides a station-level summary. For each station, the station-wise rejection rate is defined as the proportion of pairwise tests involving that station that are rejected. Larger values therefore identify stations whose latent connectivity profiles differ significantly, indicating broader reconfiguration of their connectivity patterns. When mapped geographically, the stations with high rejection rates, encoded by larger and darker points, cluster near the boundary between Brooklyn and Manhattan, separated by the East River. This spatial concentration suggests that the transition from morning to evening travel is especially pronounced for stations near waterfront areas or major inter-borough commuting corridors.

In summary, this example demonstrates the importance of statistically principled inference in network analysis. The raw estimated values may not clearly distinguish genuine structural change from ordinary estimation noise. By contrast, the inferential analysis produces much more interpretable patterns and a clearer picture of structural change. The developments in this paper could help identify credible structures and translate high-dimensional network estimates into scientifically meaningful conclusions on network connectivity patterns.

**8. Discussion.** In this work, we establish a unified framework that bridges the maximum likelihood estimator theory and practical algorithms under the latent space network models. First, we develop new theoretical results for the constrained maximum likelihood estimator that overcome the restricted eigen-gap assumption in prior analysis. Second, we address the impractical dependence on unknown ground truth in existing algorithms by introducing adaptive procedures. Specifically, for the projected gradient descent, we construct new line search conditions that can adaptively select the learning rate and prove that the explicit projection onto the unknown constraint set is unnecessary. For the universal singular value thresholding, we develop an adaptive interval for elementwise projection. Third, we prove convergence of the adaptive algorithms to the ideal constrained maximum likelihood estimator.

There are several natural generalizations based on the current results. First, the asymptotic theory in Theorem 1 focuses on a fixed set of nodes. In networks with  $n$  total nodes and  $n(n-1)/2$  edges, it is of interest to establish theoretical guarantees for simultaneous inference, such as false discovery rate control when comparing two networks, as demonstrated in the data analysis. Notably, our current asymptotic theory enables separate inference for baseline degrees and latent vectors, which form two sets of high-dimensional parameters with different interpretations. Developing unified simultaneous inference across these parameters remains an important question. Second, the framework can be extended to other model formulations. For example, when additional edgewise or nodewise covariates are available, they can be added into the network model [22] or handled via joint modeling [16, 18]. More general kernels beyond Euclidean inner products may also be considered [32]. The current arguments and asymptotic results can be generalized accordingly by updating the likelihood formulations. Third, the estimated latent vectors can be used in downstream tasks, such as regression [21] or causal inference [13]. The derived uncertainty and algorithmic approximation errors need to be properly accounted for when plugging in estimated parameters.

## SUPPLEMENTARY MATERIAL

**Supplement to “Bridging Theory and Practice: Statistical Inference of Latent Space Models for Networks”.**

Additional numerical results and proofs are deferred to the Supplementary Material.

## REFERENCES

- [1] AITCHISON, J. and SILVEY, S. D. (1958). Maximum-likelihood estimation of parameters subject to restraints. *The Annals of Mathematical Statistics* 813–828.
- [2] ATHREYA, A., PRIEBE, C. E., TANG, M., LYZINSKI, V., MARCHETTE, D. J. and SUSSMAN, D. L. (2016). A limit theorem for scaled eigenvectors of random dot product graphs. *Sankhya A* **78** 1–18.
- [3] ATHREYA, A., FISHKIND, D. E., TANG, M., PRIEBE, C. E., PARK, Y., VOGELSTEIN, J. T., LEVIN, K., LYZINSKI, V., QIN, Y. and SUSSMAN, D. L. (2018). Statistical inference on random dot product graphs: a survey. *Journal of Machine Learning Research* **18** 1–92.
- [4] ATHREYA, A., TANG, M., PARK, Y. and PRIEBE, C. E. (2021). On estimation and inference in latent structure random graphs. *Statistical Science* **36** 68–88.
- [5] BEKKER, P. A. and TEN BERGE, J. M. (1997). Generic global identification in factor analysis. *Linear Algebra and its Applications* **264** 255–263.
- [6] BRÄUNING, F. and KOOPMAN, S. J. (2020). The dynamic factor network model with an application to international trade. *Journal of Econometrics* **216** 494–515.
- [7] CAPE, J., TANG, M. and PRIEBE, C. E. (2019). The two-to-infinity norm and singular subspace geometry with applications to high-dimensional statistics. *The Annals of Statistics* **47** 2405–2439.
- [8] CHATTERJEE, S. (2015). Matrix estimation by universal singular value thresholding. *The Annals of Statistics* **43** 177–214.
- [9] CITIBIKE (2019). New York Citi Bike Data in August 2019. <https://github.com/cedoula/bikesharing>. [Original source: <https://citibikenyc.com/system-data>].
- [10] EL-HELBAWY, A. T. and HASSAN, T. (1994). On the wald, lagrangian multiplier and likelihood ratio tests when the information matrix is singular. *Journal of The Italian Statistical Society* **3** 51–60.
- [11] FANG, K., QIN, R. and FAN, X. (2025). Transfer learning under latent space model. *arXiv preprint arXiv:2509.15797*.
- [12] GOWER, J. C. and DIJKSTERHUIS, G. B. (2004). *Procrustes Problems* **30**. Oxford university press.
- [13] HAYES, A., FREDRICKSON, M. M. and LEVIN, K. (2025). Estimating Network-Mediated Causal Effects via Principal Components Network Regression. *Journal of Machine Learning Research* **26** 1–99.
- [14] HE, Y., SUN, J., TIAN, Y., YING, Z. and FENG, Y. (2025). Semiparametric modeling and analysis for longitudinal network data. *The Annals of Statistics* **53** 1406–1430.
- [15] HOFF, P. D., RAFTERY, A. E. and HANDCOCK, M. S. (2002). Latent space approaches to social network analysis. *Journal of American Statistical Association* **97** 1090–1098.
- [16] HUANG, S., SUN, J. and FENG, Y. (2024). PCABM: Pairwise Covariates-Adjusted Block Model for Community Detection. *Journal of American Statistical Association* **119** 2092–2104.
- [17] KUCHIBHOTLA, A. K. and CHAKRABORTTY, A. (2022). Moving beyond sub-Gaussianity in high-dimensional statistics: Applications in covariance estimation and linear regression. *Information and Inference: A Journal of the IMA* **11** 1389–1456.
- [18] LI, J., XU, G. and ZHU, J. (2025). High-dimensional Factor Analysis for Network-linked data. *Biometrika* asaf012.
- [19] LI, J., WU, S., CUI, C., XU, G. and ZHU, J. (2025). Statistical Inference on Latent Space Models for Network Data. *arXiv preprint arXiv:2312.06605*.
- [20] LU, C., DURANTE, D. and FRIEL, N. (2025). Zero-inflated stochastic block modelling of efficiency-security trade-offs in weighted criminal networks. *Journal of the Royal Statistical Society Series A: Statistics in Society* qnaf029.
- [21] LUNDE, R., LEVINA, E. and ZHU, J. (2023). Conformal prediction for network-assisted regression. *arXiv preprint arXiv:2302.10095*.
- [22] MA, Z., MA, Z. and YUAN, H. (2020). Universal latent space model fitting for large networks with edge covariates. *Journal of Machine Learning Research* **21** 86–152.
- [23] MA, C., WANG, K., CHI, Y. and CHEN, Y. (2019). Implicit regularization in nonconvex statistical estimation: gradient descent converges linearly for phase retrieval, matrix completion, and blind deconvolution. *Foundations of Computational Mathematics*.

- [24] MACDONALD, P. W., LEVINA, E. and ZHU, J. (2025). Latent process models for functional network data. *Journal of Machine Learning Research* **26** 1–69.
- [25] MATIAS, C. and ROBIN, S. (2014). Modeling heterogeneity in random graphs through latent space models: a selective review. *ESAIM: Proceedings and Surveys* **47** 55–74.
- [26] NAKIS, N., KOSMA, C., BRATIVNYK, A., CHATZIANASTASIS, M., EVDAIMON, I. and VAZIRGIAN-NIS, M. (2025). The signed two-space proximity model for learning representations in protein–protein interaction networks. *Bioinformatics* **41** btaf204.
- [27] NATH, S., WARREN, K. and PAUL, S. (2025). Identifying Peer Influence in Therapeutic Communities Adjusting for Latent Homophily. *The Annals of Applied Statistics* **19**. <https://doi.org/10.1214/24-AOAS1971>
- [28] NOCEDAL, J. and WRIGHT, S. J. (2006). *Numerical Optimization*, 2 ed. Springer, New York.
- [29] PAN, R., GAO, Y. and WANG, H. (2025). A latent space model for link prediction in statistical citation network. *Journal of Multivariate Analysis* 105555.
- [30] PARK, J., JIN, I. H. and JEON, M. (2023). How social networks influence human behavior: An integrated latent space approach for differential social influence. *Psychometrika* **88** 1529–1555.
- [31] ROHE, K., CHATTERJEE, S. and YU, B. (2011). Spectral clustering and the high-dimensional stochastic blockmodel. *The Annals of Statistics* **39** 1878–1915.
- [32] RUBIN-DELANCHY, P., CAPE, J., TANG, M. and PRIEBE, C. E. (2022). A statistical interpretation of spectral embedding: the generalised random dot product graph. *J. R. Stat. Soc. (Series B)* **84** 1446–1473.
- [33] SENGUPTA, S. (2025). Statistical Network Analysis: Past, Present, and Future. In *Frontiers of Statistics and Data Science* 153–179. Springer.
- [34] SMITH, A. L., ASTA, D. M. and CALDER, C. A. (2019). The geometry of continuous latent space models for network data. *Statistical Science: a Review Journal of the Institute of Mathematical Statistics* **34** 428.
- [35] SUSSMAN, D. L., TANG, M. and PRIEBE, C. E. (2013). Consistent latent position estimation and vertex classification for random dot product graphs. *IEEE Transactions on Pattern Analysis and Machine Intelligence* **36** 48–57.
- [36] TANG, M. and PRIEBE, C. E. (2018). Limit theorems for eigenvectors of the normalized Laplacian for random graphs. *The Annals of Statistics* **46** 2360–2411.
- [37] TANG, M., ATHREYA, A., SUSSMAN, D. L., LYZINSKI, V. and PRIEBE, C. E. (2017a). A nonparametric two-sample hypothesis testing problem for random graphs. *Journal of Computational and Graphical Statistics* **26** 344–354.
- [38] TANG, M., ATHREYA, A., SUSSMAN, D. L., LYZINSKI, V., PARK, Y. and PRIEBE, C. E. (2017b). A semiparametric two-sample hypothesis testing problem for random graphs. *Journal of Computational and Graphical Statistics* **26** 344–354.
- [39] TEN BERGE, J. M. (1977). Orthogonal Procrustes rotation for two or more matrices. *Psychometrika* **42** 267–276.
- [40] TIAN, Y., SUN, J. and HE, Y. (2025). Efficient Analysis of Latent Spaces in Heterogeneous Networks. *Journal of the American Statistical Association*. <https://doi.org/10.1080/01621459.2025.2604316>
- [41] TU, S., BO CZAR, R., SIMCHOWITZ, M., SOLTANOLKOTABI, M. and RECHT, B. (2016). Low-rank solutions of linear matrix equations via procrustes flow. In *International Conference on Machine Learning* **48** 964–973. PMLR.
- [42] VAN DER VAART, A. W. (2000). *Asymptotic Statistics* **3**. Cambridge university press.
- [43] VLADIMIROVA, M., GIRARD, S., NGUYEN, H. and ARBEL, J. (2020). Sub-Weibull distributions: Generalizing sub-Gaussian and sub-Exponential properties to heavier tailed distributions. *Stat* **9** e318.
- [44] WANG, F. (2022). Maximum likelihood estimation and inference for high dimensional generalized factor models with application to factor-augmented regressions. *Journal of Econometrics* **229** 180–200.
- [45] WANG, Y. and GUO, Y. (2023). LOCUS: A regularized blind source separation method with low-rank structure for investigating brain connectivity. *The Annals of Applied Statistics* **17** 1307.
- [46] WANG, S., WANG, Y., XU, F., SHEN, L. and ZHAO, Y. (2024). Sex-specific topological structure associated with dementia identified via latent space network analysis. *Alzheimer's & Dementia* **20** e090404.
- [47] XIE, F. and XU, Y. (2023). Efficient estimation for random dot product graphs via a one-step procedure. *Journal of American Statistical Association* **118** 651–664.
- [48] YOUNG, S. J. and SCHEINERMAN, E. R. (2007). Random dot product graph models for social networks. In *Proc. Int. Workshop Alg. Models Web-Graph* 138–149. Springer.
- [49] ZHANG, X., XUE, S. and ZHU, J. (2020). A flexible latent space model for multilayer networks. In *International Conference on Machine Learning* **119** 11288–11297. PMLR.
- [50] ZHAO, Y., LEVINA, E. and ZHU, J. (2012). Consistency of community detection in networks under degree-corrected stochastic block models. *The Annals of Statistics* **40** 2266–2292.